ISSN 1905-9094

GMSARN INTERNATIONAL JOURNAL

Vol. 6 No. 1
March 2012

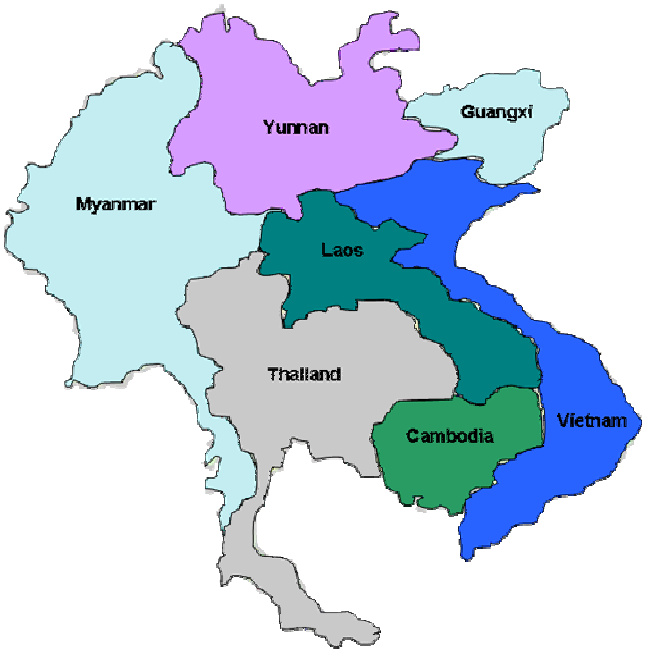

Published by the

GREATER MEKONG SUBREGION ACADEMIC AND RESEARCH NETWORK
c/o Asian Institute of Technology
P.O. Box 4, Klong Luang, Pathumthani 12120, Thailand

GMSARN INTERNATIONAL JOURNAL

GMSARN MEMBERS

Asian Institute of Technology	P.O. Box 4, Klong Luang, Pathumthani 12120, Thailand. www.ait.asia
Guangxi University	100, Daxue Road, Nanning, Guangxi, CHINA www.gxu.edu.cn
Hanoi University of Technology	No. 1, Daicoviet Street, Hanoi, Vietnam S.R. www.hut.edu.vn
Ho Chi Minh City University of Technology	268 Ly Thuong Kiet Street, District 10, Ho Chi Minh City, Vietnam. www.hcmut.edu.vn
Institute of Technology of Cambodia	BP 86 Blvd. Pochentong, Phnom Penh, Cambodia. www.itc.edu.kh
Khon Kaen University	123 Mittraparb Road, Amphur Muang, Khon Kaen, Thailand. www.kku.ac.th
Kunming University of Science and Technology	121 Street, Kunming P.O. 650093, Yunnan, China. www.kmust.edu.cn
National University of Laos	P.O. Box 3166, Vientiane Perfecture, Lao PDR. www.nuol.edu.la
Royal University of Phnom Penh	Russian Federation Blvd, PO Box 2640 Phnom Penh, Cambodia. www.rupp.edu.kh
Thammasat University	P.O. Box 22, Thamamasat Rangsit Post Office, Bangkok 12121, Thailand. www.tu.ac.th
Yangon Technological University	Gyogone, Insein P.O. Yangon, Myanmar
Yunnan University	2 Cuihu Bei Road Kunming, 650091, Yunnan Province, China. www.ynu.edu.cn

ASSOCIATE MEMBERS

Chulalongkorn University	254 Phayathai Road, Pathumwan, Bangkok, 10300, THAILAND www.chula.ac.th
Mekong River Commission	P.O. Box 6101, Unit 18 Ban Sithane Neua, Sikhottabong District, Vientiane 01000, LAO PDR www.mrcmekong.org
Nakhon Phanom University	330 Apibanbuncha Road, Nai Muang Sub-District, Nakhon Phanom 48000, THAILAND www.npu.ac.th
Ubon Ratchathani University	85 Sathollmark Rd. Warinchamrap Ubon Ratchathani 34190, THAILAND www.ubu.ac.th

GMSARN
INTERNATIONAL JOURNAL

GREATER MEKONG SUBREGION ACADEMIC AND RESEARCH NETWORK (http://www.gmsarn.org)

The Greater Mekong Subregion (GMS) consists of Cambodia, China (Yunnan & Guangxi Provinces), Laos, Myanmar, Thailand and Vietnam.

The Greater Mekong Subregion Academic and Research Network (GMSARN) was founded followed an agreement among the founding GMS country institutions signed on 26 January 2001, based on resolutions reached at the Greater Mekong Subregional Development Workshop held in Bangkok, Thailand, on 10 - 11 November 1999. GMSARN was composed of eleven of the region's top-ranking academic and research institutions. GMSARN carries out activities in the following areas: human resources development, joint research, and dissemination of information and intellectual assets generated in the GMS. GMSARN seeks to ensure that the holistic intellectual knowledge and assets generated, developed and maintained are shared by organizations within the region. Primary emphasis is placed on complementary linkages between technological and socio-economic development issues. Currently, GMSARN is sponsored by Royal Thai Government.

The GMSARN current member institutions are the Asian Institute of Technology, Pathumthani, Thailand; The Institute of Technology of Cambodia, Phnom Penh, Cambodia; Kunming University of Science and Technology, Yunnan Province, China; National University of Laos, Vientiane, Laos PDR; Yangon Technological University, Yangon, Myanmar; Khon Kaen University, Khon Kaen Province, Thailand; Thammasat University, Bangkok, Thailand; Hanoi University of Technology, Hanoi, Vietnam; Ho Chi Minh City University of Technology, Ho Chi Minh City, Vietnam; The Royal University of Phnom Penh, Phnom Penh, Cambodia; Yunnan University, Yunnan Province and Guangxi University, Guangxi Province, China; and other associate members are Chulalongkorn University, Bangkok, Thailand; Mekong River Commission, Vientiane, Laos PDR; Nakhon Phanom University, Nakon Phanom Province, Thailand; and Ubon Ratchathani University, Ubon Ratchathani Province, Thailand.

GMSARN International Journal

Volume 6, Number 1, March 2012

CONTENTS

The Costs of Power Quality Disturbances for Industries Related Fabricated Metal, Machines and Equipment in Thailand

Panuwat Teansri, Worapong Pairindra, Narongkorn Uthathip
Pornrapeepat Bhasaputra, and Woraratana Pattaraprakorn

Abstract— *The purpose of this paperis to examine industrial customer attitudes relating impacts from power quality events which include voltage sags, undervoltage, overvoltage and voltage interruption. In this study, 63 industries associated fabricated metal, machines and equipment products in Nava Nakorn industrial zoneare selected to estimatemonetary losses from power quality events in 2010. The direct customer survey with questionnaire guideline is introduced in the data collecting process.In the survey questionnaire, customer attitudes are represented in term of impacts levels to manufacturing processes and thier activities. The economic impact level is then transformed into monetary value by using weighting economic factor. The customer survey results show that the impact level from each power quality event is diversified. It is significantly related to conditions of production capacity, product values, manufacturing processes, amount of sensitive devices and plant recovery time. In addition, the manufacturing industries of semiconductors, integrated circuit (IC) and electronic products perceived a large of monetary losses in case of power quality event and as well as voltage interruption.However, power quality monitoring system, a tool for identifying power quality problems, is still not available in some industries. Further, various industries in this survey never perform full assessment of manufacturingimpacts. Therefore,the economic impact calculationis employed based on industrial expert experiances. The results in this studyare information from customer attitudes related to reliability cost which utility planners can be applied in various fields of electric distribution system including operation, maintenance and network improvementplanning. Finally, the assessment is introduced for industries to address issues about the consequnces ofpower quality problems and reliablity of power supply.*

***Keywords*— Power quality, Voltage sag, Voltage interruption, Fabricated metal, machines and equipment industry.**

1. INTRODUCTION

Currently, numerous developments in power system technologies are widely utilized in electric power industry and customers. Various loads equipment based microprocessor controllerand power electronic devices arealso more sensitive to power quality.Further, improvements on overall power system efficiency from both supply and demand sides resulted in growth ofsensitive devices such asautomatic control system, high efficiency machines, adjustablespeed drives (ASD) and shunt capacitors. This is resulting in concerns about the future impact on system capabilities. Moreover, customers have an increased awareness power quality issues which are becoming better informed from driven factors in power system restructuring and deregulation of power utility industry. Therefore, electric utilities in several countries have been collaborated with their customersto evaluate the impacts from powerquality event. The results of customer impact evaluation can be applied for identifying the optimalmigrationalternatives.

Since the key factor ofnational economic growth and social developmentin developing countries,energy utilization in Fig. 1 shows that industrial sector is the largest consumer in Thailand with share 42.40% of total electrical energy consumption in 2009.In addition, value added contribution from nine industrial sectorsin Fig. 2 displays that industries related to fabricated metal, machines and equipment (TSIC38) is the highest contributor of gross domestic product (GDP) for industrial sector, followed by the food industries (TSIC 31) and textile industries (TSIC 32), respectively.Due to a variety of products and value added contribution, this paper intends to estimateeconomic impacts from power quality problems of industries under TSIC 38.

2. LITERATURE REVIEW

The power quality has become an issue of increasing interest in the various segments of end user since the late of 1980s. At that time, the dominated cause of power quality problems is from natural phenomena and then thegrowth of non linear loads in several applications is extended into a power quality of harmonics problem. Table 1 provides information regarding characteristics

Panuwat Teansriis the doctoral student in the field of Electrical Engineering, the Department of Electrical and Computer Engineering, Faculty of Engineering, Thammasat University, Pathumthani, Thailand. E-mail: panuwat.teansri@hotmail.com.

Worapong Pairindrais the doctoral student in the field of Electrical Engineering, the Department of Electrical and Computer Engineering, Faculty of Engineering, Thammasat University, Pathumthani, Thailand. E-mail: worapong.pa@spu.ac.th.

Narongkorn Uthathipis the master student in the field of Electrical Engineering, the Department of Electrical and Computer Engineering, Faculty of Engineering, Thammasat University, Thailand. E-mail: tae_satul@hotmail.com.

Pornrapeepat Bhasaputrais with the department of Electrical and Computer Engineering, Faculty of Engineering, Thammasat University, 99 M. 18Phahoyothin Road, Khongluang, Pathumthani 12120, Thailand E-mail: bporr@engr.tu.ac.th.

Woraratana Pattaraprakornis with the department of Chemical Engineering, Faculty of Engineering, Thammasat University, 99 M 18Phahoyothin Road, Khongluang, Pathumthani 12120, Thailand E-mail: pworarat@engr.tu.ac.th.

and causes of common power quality problems. Equipment may have different sensitivity to power quality problems which dependon the specific load type, control setting and application. Consequently, it is often difficult to identify characteristics of problems when power quality monitoring system is not installed in a factory.

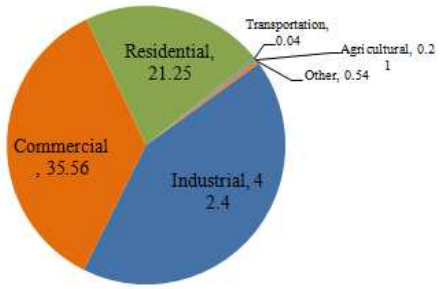

Fig. 1. The electrical energy consumption in 2009.

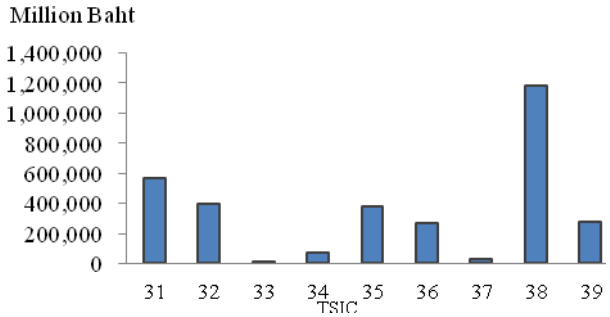

Fig. 2. GDP originating frommanufacturing in 2008.

Table 1.Categories of power quality problems

Characteristics	Causes
Momentary interruption	- Short circuit, operation of protective devices such as breaker and fuse
Temporary interruption	- Short circuit, operation of protective devices
Sustain interruption	- System short circuit, accidents, tree falling
Notch	- Commutated current by operation of power electronic devices
Transient (Impulsive/Oscillatory)	- Lightning, system fault, switching of heavy load such as induction motor starting
Sag	- System faults, switching of heavy load, motor starting
Swell	- Remote system fault, switching off a large load capacitor bank
Undervoltage	- Large load or system switching, faulty connection or wiring and loose connection connections
Overvoltage	- Load switching such as switching off large load or system switching on a large capacitor bank, incorrect tap settings on transformers

In general, power quality problems can be categorized in different standards accordingto development objectives or criteria of typical duration, voltage magnitude and frequency content. For instance, the general proposes of power quality standard development include IEEE standard 1159 [1], the IEEE Standard 519-1992 [2], IEC 61000-4-30 [3] while the SEMI Standard F-47 is developed for specific propose to serve manufacturers and suppliers of hardware, ICT services and software [4].The IEEE Standard 1159 was developed to provide general guidelines forpower standard definitions and quality measurements in different categories of power quality events while the IEEE Standard 519-1992was designed to establish guidelines for harmonic current and voltage distortionlevels on distribution and transmission circuitsand the IEC 61000-4-30 was set up to define the correct measuring algorithms for power quality instruments. In addition, the customer load model can also be used as the method to analyze the power quality events, however load diversify and time-dependent operation makes this approach impracticable. Instead, equipment sensitivity to power quality can be considered in the power acceptability curve. One of thewidely well-known curves is Computer Business Equipment Manufacturers Association (CBEMA) [5].

Since the association reorganized in 1994 and was subsequently renamed the Information Technology Industry Council (ITI), the CBEMA curve was also updated and renamed the ITI curve. Typical loads will likely trip off when the voltage is below the CBEMA or ITI curve like a sample application for setting run/stop of load in Fig. 3. The curve labeled ASD represents an example of voltage sag ride through capability for a device that is very sensitive to voltage sags. It trips for sags below 0.9 p.u. that last for only 4 cycles. The motor contactor curve represents typical contactor sag ride-through characteristics. It trips for voltage sags below 0.5 p.u. that last for more than 1 cycle.

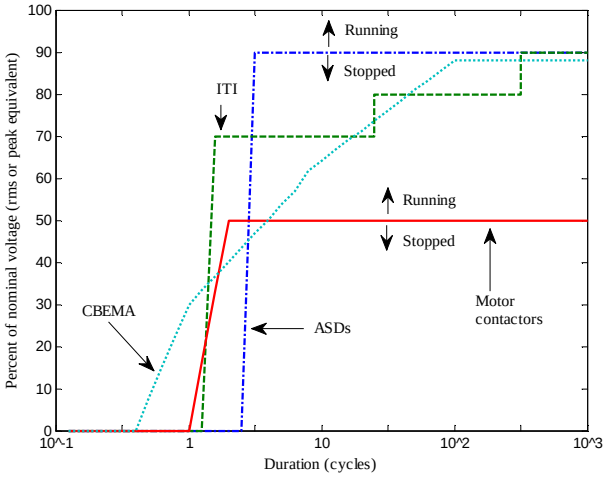

Fig. 3.Equipment voltage sag ride-through capability curves.

In electricity market, power quality is interested by electric utility companies, equipmentmanufacturers and electric power customers. There aremany reasons associated concerns which comprising of economic growth, rising rapidly in electricity demand, modern and advance technology developments of sensitive devices, customer service standard. For these reasons, numerous researches related power quality problems analysis, monitoring systems, mitigation methods, technical standards, and economic impact evaluations are continue to publish. The study results related to power quality issues led to establishment power quality indices in regulation of service standard for worldwide countries [6-11]. In addition, evaluation of power quality cost especially industrial sector was performed at the beginning of the 1990s for comparing with the cost of power quality services. The survey of industrial customers contribute on underlining the power quality disturbances susceptibility of industrial processes and also giving the estimation of annual costs experienced by customers[12]. The cost of a disturbance involves losses from lost production, damaged raw material, idle labors and in certain cases damaged equipment. The IEEE standard 1346–1998 provides some guidelines on how to calculate thecost associated a voltage disturbance which the approach requires participation of management as well as financial,operational, maintenance, and sales staffs [13]. However, some utilities face resources limitation and it is so difficult in practical to interview all participants at the same time. Some first study to assess the power quality cost was performed in USA and Canada [14-15]. The customer damage from power quality events can impact from microeconomic to macroeconomic in these countries. For instance, a feeder with high number of short interruption and voltage sag was estimated losses by 1.8 Million US$ [16]. In Italy, the survey of economic impacts in manufacturers from power quality problems was evaluated in range of 50-250,000 US$ per year per factory [17]. In South Africa, a recent study showed that major industries suffer annual losses of more than 200 US$ million due to voltage sag problems [18]. The survey results of European-wide in 2007 suggested that several companies lost up to 10% of their annual turnover due to poor power quality [19]. For industrial perspectives, the effects of power quality on weaving-knitting, dyeing and finishing processes in textile industry were assessed in term of partial interruption, major interruption and complete breakdown to textile processes. The results of power quality measurement showed that losses were significantly high, being around 15% of the annual net profit of the textile industry [20]. In automotive industry, four-cycle voltage sag can lost over 700,000 US$ in the following 72 minutes due to shut down of process and required rework from malfunction of programmable controllers and drive systems working in a real-time process environment [21]. The high technology machines of semiconductor companies in Taiwan including wafer manufacturing and integrated circuit packing identified that losses due to power quality event was greater than 5 million NT$ per event (1US$=28.66NT$) [22]. Another estimation the losses of semiconductor manufacturing was conducted in Iran [23]. The economic impact caused by voltage sag was shutdown production processes of 23 minutes which the company suffered losses about 138,000 US$. This evaluation may greater losses when include equipment and machines damage costs, reduced product quality, increased maintenance costs. For chemical industry, 20,053 pharmaceutical manufacturing companies in India were investigated economic impacts from poor power quality in 2009. The total cost of complete plant disruption including direct costs, downtime costs and restart processes costs due to all power quality events for worst case scenario was approximately Rs.20 billion (1 US$=26.474 Rs at June 2009). The losses from voltage disturbances alone accounts for 50% of the total cost of downtime due to all events. This results were calculated the cost of downtime due to all events and voltage disturbances alone, account for 10.33% and 5.16% of the national annual production of pharmaceutical companies, respectively [24]. The power quality costs due to voltage sag in various industries were estimated as shown in Table 2 [25]. This literature is also addressed the survey results of Frost and Sullivan, an independent consulting firm specializing in evaluating technology markets, about cost of voltage disturbances alone impact to US industry over 20 billion US$ every year. Since the power quality in Thailand is less attention to study problems, causes and impacts, the paper has been examined the customer attitudes related to manufacturing processes affected from power quality and interruption statistics in 2010. Impacts of voltage sags, undervoltage and overvoltage are presented in this study.

Table 2. Impact of voltage sags on industries

Industry	Losses (US$)
Semiconductor industry	2,500,000
Credit card processing	250,000
Equipment manufacturing	100,000
Automobile industry	75,000
Chemical industry	30,000

3. METHODOLOGY

The research of economic impacts from power quality problems is still less attention especially in developing countries. In addition, power service standardsare defined only power supply reliability indices such as the system average interruption frequency index (SAIFI) and the system average interruption duration index (SAIDI). In this study, the methodology to assess power quality costs from industrial customer perspectives is developed based on customer survey. The questionnaire is developed from several guidelines and publications to fulfill the customer information and relevant data. The contents of survey questionnaire are divided into four parts as following:

Part I: *General manufacturing information*; this part is formed to obtain data includes factory location, manufacturing processes, type of activity, number of employees, operating time in a day and in a week, and data on the electric end-use (voltage level, demand and average electrical energy consumption). In addition, personal contact information such as name of respondent, mobile phone number, fax number, e-mail address isalso defined in this section.

Part II: *List of sensitive devices*; information about sensitiveloads, equipment and machines in industrial processes including programmable logic *controllers* (PLC),automation control system, ASD, soft starters, computerized numerical control (CNC), computers, power electronic devices, switching power supply, power rectifier, magnetic contactors is filled in the survey questionnaire. Further, respondents were asked to describe different impact between power quality problems (voltage sag) and zero-voltage condition (sustain interruption).

Part III: *Cost of power quality problems*; impact level from each power quality categorycomprising instantaneousvoltage sag, momentary voltage sag, temporary voltage sag, under voltage, over voltage and sustained interruption is estimated. Data on each impact level provides qualitative costsat specific impact level (not impact to complete process shutdown). In this case, customer impacts from sustain interruption is assigned as the reference cost. The power quality costs referred to the impact from voltage sags can be calculated by using weighting economic factor.

Part IV: *Power quality events in a year*; the statistic data of power quality problems occurred in 2009provided by monitoring system or manual documentation system is collected.

4. THE SURVEY ORGANIZATION

Due to high density of industrial customer located on the logistic hubfor productsdistribution, the industries operating in Nava Nakornindustrial zone are the target groupof survey.Over 217 industries and more 200,000 employees are currently operating in this industrial zone. The industries utilizeelectricity from distribution utility,namely the Provincial Electricity Authority (PEA). The electricity supply to industries consists of 4 main substations, each connected with 10 feeders. A total capacity from 4 substations was desired at 515 MVA and connected in loop circuit to prevent electric problems. The specification of electric substation system is summarized in Table 3which the distribution utility delivers electricity with the medium voltage of 115 kV and 22 kV.For industrial information, the number of industry in each category is shown in Table 4. The statistic data shows that 120 factories related to fabricated metal, machines and equipment (TSIC 38) is the highest number of industry in Nava Nakhon industrial zone. In this industrial category, several products are the majority contributorto national economy. Considering production process, most of manufacturing industries under TSIC 38 operate with high technology machines and sensitive devices includingautomatic control system, electronic control cards and vary speed drive controlled motors. Poor power quality may damage the system andcause all production lines failures. Thus, the scope of this study is to investigate the economic value of various industries under TSIC 38from power quality disturbances.The study has been carried out by interview expert in the factory to address level of impactin each power quality category. The costs of power quality event can be estimated with the weighting factors in Table 5 that refer to the cost of sustain interruption.

Table 3. Electric substation capacity in Nava Nakorn industrial zone

Substation	Code	Supply capacity (MVA)	Rated voltage (kV)
Nava Nakorn 1	NVA	2x40	115/22
Nava Nakorn 2	NVB	2x40	115/22
Nava Nakorn 3	NVC	2x50	115/22
Nave Nakorn 4	NVD	2x40	115/22

Table 4. Number of industry in Nana Nakorn industrial zone classified by TSIC

TSIC	Description	Number of industry
31	Food, beverage and tobacco	19
32	Textile and apparel	8
33	Wood and wood products	5
34	Pulp and paper	6
35	Chemical and petrochemical products	38
36	Non metallic mineral	3
37	Basic metal	3
38	Fabricated metal, machines and	120
39	Other manufacturing	15
Total		**217**

Table 5.The guideline of qualitative impact level and economic impact weighting of power quality problems

Level of impact	Weighting for economic analysis	Guideline
No effect	0.0	All processes not impact, short process recovery time and there is no raw material damages
Very less impact (sag with minimum voltage between 70% and 90%	0.1	Most processes not impact. However, some processes which not critical may impact during voltage sag
Less impact (sag with minimum voltage between 50% and 70%)	0.3	Some processes have been stopped while othersare still normal operation. However, overall production lines cannot full operation capacity.
Medium to quite large impact (sag with minimum voltage below 50%)	0.5-0.7	Most processes were interrupted. Long recovery times at least half an hour was normally required to check machine breakdown and then restart process.
Large to greatest impact (short and long interruption)	0.8-1.0	Most processes interrupted and consequence of completedproduction lines shutdown. Long recovery time is required to inspect material damages, machines breakdown and then restart processes.
Cannot identified	N/A	Never investigate or not install power quality monitoring system

5. STUDY RESULTS

5.1 General industrial customer survey information

Regarding the highest number of industry in Nava Nakorn industrial zone,120 companies related to fabricated metal, machines and equipment products are selected as the target to estimate costs of power quality event and voltage interruption. The data gathering process was achieved by direct customer interviews in case of industries preference or the questionnaire response in case of an industry does not prefer to reveal plant information. Although survey information is given by experts in manufacturing processes or well-known person about electric power system in the factory, there are some industries which the survey information in questionnaire was not useful or may not represent to the generalized results. After validating responded data, 63industriesare represented in the analysis and evaluation costs associated power quality event. The selected data from customer survey can be classified into sub-category under TSIC 38 as shown in Table 6. Overall response rate is approximately with 52.5% of total industry. In this survey, the industry related to equipment, radio, television and communication products (TSIC38320) have the largest number of respondents, followed by automotive parts and general assembly industry (TSIC 38439). The description and example products under each sub-category can be summarized in Table 7.

Table 6. Sample size and number of responses

TSIC	Population	Respondent	Response rate (%)
38110	5	1	20
38198	5	2	40
38500	5	2	40
38199	5	5	100
32220	5	1	20
38240	5	3	60
38292	5	3	60
38320	30	23	76
38330	10	2	20
38393	10	2	20
38399	5	2	40
38250	10	5	50
38439	20	12	60
Total	120	63	52.5

Table 7. List of sub-category under fabricated metal, machines and equipment industry (TSIC 38)

TSIC	Description	Examples of products
38110	Factories related cutlery tools and appliances made of steel	cutting wheel
38198	Factories related coating, engraving services and related services grew	mold for die casting
38220	Factories related machinery and agricultural equipment	Small diesel engine, walk-behind tractor rice reaper tractor, oil & spare parts
38240	Factories related machinery and special equipment for industrial applications	electric discharged machine, wire-cut, machine centers injection mold machine
38292	Factories related air conditioning systems	parts of air condition (strainer, header assembly, distributor, reducer pipe)
38320	Factories related equipment and radio, television and communication	color television, video, CCTV, VTR ,Satellite Receiver Equipments
38330	Factories related machinery and home appliances that use electricity	electrical appliances (washing machine, cooker, refrigerator, etc.)
38393	Factories related electric lamps and lighting systems	automotive lighting equipment
38399	Factories related other electrical equipments	transformers,heat exchanger,defrost heater,thermostat vend-mechanism and water pump
38250	Factories related theelectronic and computer assembly parts	computer hard-disk , flexible printed circuit board, transistor, diodes,resisters, capacitors, integrate circuits (IC)
38439	Factories related the automotive industry, parts and assembly	gear set for motorcycle
38500	Factories related the equipment measurement and control profession	clamp meter,multi meter,wall clock, alarm clock, table clock
38199	Factories related fabricated metal products which are not classified in the other	

Considering industrial scale by using electrical energy consumption criteria from electricity tariff structure of the Provincial Electricity Authority (PEA), the survey shows that large scale industries which consumed average electricity more than 250,000 kWh a month is the highest participant for this study (33 factories), however medium scale industries (electricity consumption between 100,000-250,000 kWh a month) and small scale industries (less than 100,000 kWh a month) also response significantly as shown in Fig. 4.Distribution of electrical energy consumption is also plotted in Fig. 5 which the two-largest electrical energy consumers are from the manufacturing of semiconductors including various types of IC, passive module, discrete semiconductors and optoelectronics products, followed with hard disk drive manufacturing, respectively. When filtering the two-largest energy consumers out of samples as Fig. 5 (below), a half of remaining industries consume electricity in a range of 100,000-1,000,000 kWh per month with the average of 346,492 kWh per month. Information about electricity consumption reveals that most industries categorized in TSIC 38 and located in Nava Nakorn industrial zone are large general service business sector under electricity tariff structure of PEA.

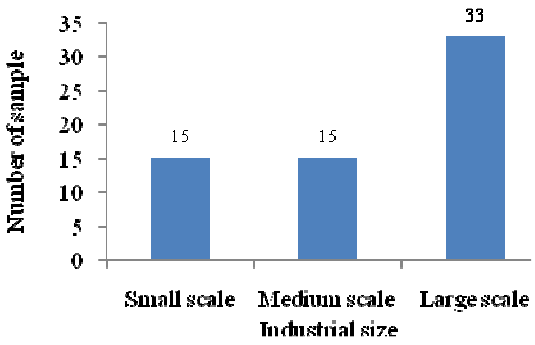

Fig. 4.Industrialrespondents categorized by scale.

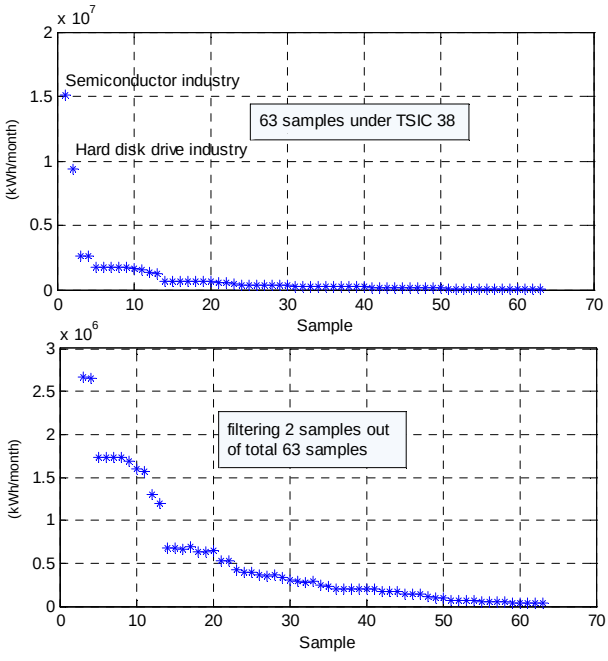

Fig.5. Scatter plot of electrical energy consumption.

To increase respondents understanding of the different impacts between power quality problem and reliability problem, the customers were asked their experiances about power quality problems in a year and how they can identify which problem was from power quality? The guideline for customer survey in this question is “the factory has been set up power quality monitoring or not?” In case the power quality monitoring system was not installed especially in a small scale industry, the customer were asked the experiances about protective devices malfunction such as main circuit breaker tripped from unknow reason while electric network was still in normal condition. In addition, the customers were asked to inform the overal processes impact from power quality and from power interruption. The survey results show that most industrial customersperceived a different impact between sustain interruption and power quality problem while the remaining indicated an equal impact. In general, the factories with continuous processes require a time to restart all processes since most production lines are driven by sensitive devices, machines and equipment. After voltage sag or power interruption has been activated, the production lines need to reset and investigate the material damage before restart process again. Based on survey questionnaire, Table 8providesinformation of installed devices, equipment and machines which sensitive to power quality problemsfor industries under TSIC 38.

Table 8. Installed sensitive devices, machines and quipment of manufacturing in selected industry

Sensitive devices, machines and equipment	Proportional (%)
Power electronics devices (ASD)	58.73
Computer and IT system	65.08
Switching power supply, rectifier, PLC	73.01
Magnetic contactor for motor control	73.01

Due to a variety of products, the results of customer survey show that most process characteristics of industries under TSIC 38were driven based on hand-made operation and inspection. Human resources are essential factor for a factory to make products. However, some industries have a semi-continuous processes that mean some parts of products can be completed by automation system while assembly process and final inspection arestill required human resources. The application of power electronic devices such as VSDnot widely apply in production lines while process automation system and magnetic contactorfor motor operation control are common utilized in most industries.

5.2 Economic impacts of power quality disturbances from industrial expert perspectives

Considering economic impacts from various power quality problems including instantanous sag, momentary sag, temporary sag, undervoltage, overvoltage and sustain interruption, the survey results are summarized in Fig.6 to Fig.11, respectively.

From sensitivity of equipment and process controls, the customer survey conclude that advance technology industry especially the processes of semiconductor fabrications require high levels of power quality. A case of 0.2 second voltage sag, a class of instantanous sag, can activate emergency off on various tools and cause productions lines to go down for hours.From the specifying impact level in case of instantaneousvoltage sag in Fig.6 (the rms voltage decreases to between 0.1 and 0.9 p.u. for a duration time of 0.00833 second to 0.5 second), the highest number of industryis in the level of low impact while 8 industries indicate that instantaous voltage sag affected equal to zero-voltage conditions. However, this event was rarely occurred in the network.

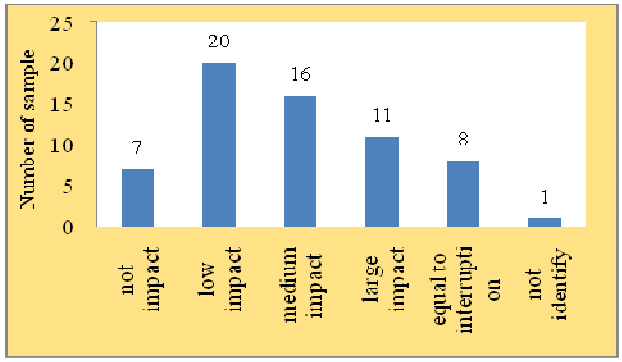

Fig. 6. Impact level of instantaneousvoltage sag.

The specifying impact level of momentaryvoltage sag is shown in Fig. 7 (the rms voltage decreases to between 0.1 and 0.9 p.u. for a time duration of 0.5 second to 3 second). The 20 industries from survey indicate that they haveperceiveda large impact from momentary voltage sag while 11 industries had experiences of losses equal to voltage interruption. Most of a large economic impact is in large scale semiconductor industry.

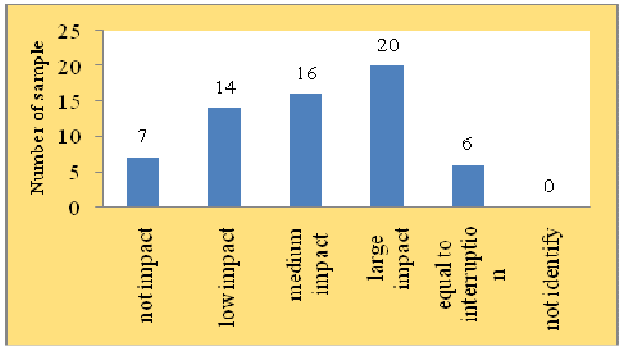

Fig. 7.Impact level of momentaryvoltage sag.

Further, the impact levels of temporary voltage sag are assessed as shown in Fig. 8 (the rms voltage decreases to between 0.1 and 0.9 p.u. for a time duration of 3 to 60 seconds). The survey shows that industries had a large impact when temporary voltage sag wasoccurred. The economic impacts from instantaneous, momentary and temporary voltage sag imply that duration is significant to impact levels. The average value of impact levels from voltage sags is used to estimate the costs of power quality.

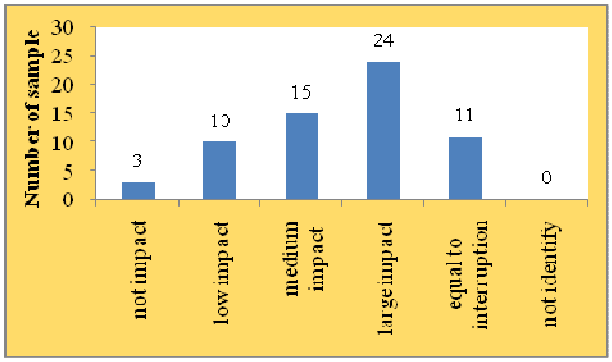

Fig. 8.Impact level of temporary sag.

For the case of undervoltage which rms voltage decreases to between 0.8 and 0.9 p.u. for a period of time greater than 1 minute, distribution of economic impact level from customer survey is shown Fig. 9. Most of undervoltage can be the result of load switching.Consequently,process machines and equipment might have operation malfunction. For instance, typical setting motor controller with 70-80% of norminal voltage cause an increasing heating loss in induction motor during long duration undervoltage. However, in this survey, the power quality event in case of undervoltagewasnot frequently happened since large loads were not applied in the industries. Fig. 10 illustrates customer attitudes about economic impact level from overvoltage which the magnitude of voltage is between 1.1-1.2 p.u. for duration longer than 1 minute. Overvoltage can be the similar causestoundervoltage. It may cause of immediate equipment failure especially electronic devices. Electric transformers and power cable of rotating machines can result in loss of equipment life time. From daily inspection, an overvoltage event ismore attended to concerndue to energy saving program in several factories. Forundervoltage and overvoltage problems, respondents indicate that economic impacts can vary from medium level to the damage equal to zero-voltage conditions. It reveals that most industrial processescan serious impact from undervoltage and overvoltage more than voltage sag.

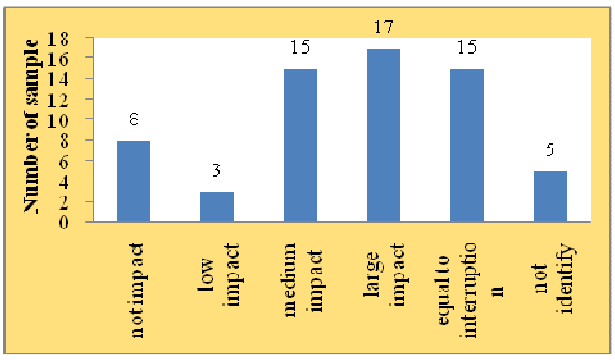

Fig. 9. Specifying impact level of undervoltage.

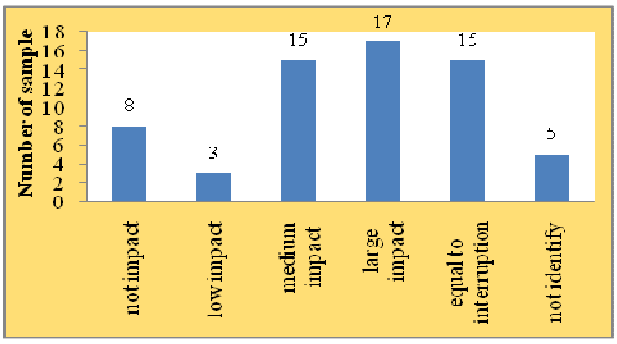

Fig. 10. Specifying impact level of overvoltage.

In addition, the specifying impact levels of sustain interruption (duration longer than 1 minute) are surveyed which the result is shown in Fig. 11. Most respondents informed that unreliable power relating sustain voltage interruption can contribute to a large economic impact. The voltage interruption is caused by the operation of protective devices such as breakers tripping and fusesblown out. In this industrial area, industrial customershadexperiences about 9 sustain interruptions and 18 events of recloser operation. Industrial process interruptions were caused by a wide range of phenomena includingequipment failures, animals, trees, severe weather, and human error. However, the statistic of interruption indicates that the majority of causes are from equipment failures. Regarding power quality and reliability improvement programs, the distribution utility who responsible in this service area has a great challenges opportunity to improve the network performance for minimizing industrial customer impacts and increasing customer satisfaction.

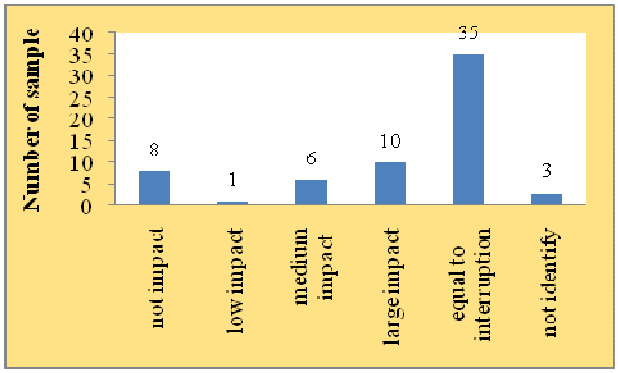

Fig. 11. Specifying impact level of sustain interruption.

5.3 Estimation cost of power quality problems

In order to estimate the costs of power quality problems, the weighting factors in Table 5are applied for calculation which the cost of voltage interruption was used as the reference value.The estimation of costs is divided into three industrial scale comprising small scale industry, medium scale industry and large scale industry, respectively. The calculation results in term of monetarylosses per event and monetary losses per average demand are summarized in Table9 and Table 10, respectively. Power quality costs in case of voltage sag

varied from 20,833 to 335,290 Baht per event imply that industrial scale is significant to the losses from power quality.Further, the power quality cost of this survey is approximate 60-70% with respect to the cost of sustain interruption. The calculation results revealed that power quality problems are important issue for industrial customers as well as the voltage interruption.

Table 9. Power quality costs based event of problems

Scale	Voltage sag		Voltage Interruption	
	Baht/event	US$/event	Baht/event	US$/event
Small scale	20,833	637.47	32,667	999.57
Medium scale	37,875	1,158.93	52,000	1591.13
Large scale	335,290	10,259.49	503,935	15419.81

Remark: 1 US$≈32.681 Baht (2010)

Table 10. Power quality costs based customer demand

Scale	Voltage sag		Voltage Interruption	
	Baht/kW	US$/kW	Baht/kW	US$/kW
Small scale	125.64	3.84	207.96	6.36
Medium scale	34.27	1.04	85.53	2.61
Large scale	119.82	3.67	180.09	5.51

Remark: 1 US$ = 32.6810 Baht (2010)

6. CONCLUSION

Modern technology industry has extremely high value productionprocesses which are more sensitive to power quality events.This paperpresents the survey results about power quality costs and voltage interruption costs of 63 advance technology industries related to fabricated metal, machines and equipment products.The selected industries were located in Nava Nakorn industrial zone, Pathumthani province, Thailand. Regarding to thestatistic of circuit breaker and recloser operations in 2010, industries in the areahad experiencedof economic losses from both direct and indirect costs. The levels of customer impact are dependent to significant factors including types of the power quality problems, value of products, manufacturing processes, industrial size or capacity and etc,. High level of customer impact is categorized in large scale industry especially in semiconductors, hard drives and computer components products. The economic impact levels from various power quality categories wereestimated by industrial expert experiences stated inquestionnaire guideline. In case of voltage sag, the average monetary losses are evaluated with 20,833, 37,875 and335,290Bahtper event for small scale industry, medium scale industry and large scale industry, respectively.In addition to reliability aspects, the industrial impact associated sustain voltage interruption can be evaluated with 32,667, 52,000 and 503,935Baht per event for small scale industry, medium scale industry and large scale industry, respectively. The estimation reveals that it is important to consider the impacts of both interruptions and power quality problems. Based on customer survey results, installation monitoring system is the basic measure for industries to deal with power quality and reliability problems. The conditions of quality and reliability of power supply can accelerate or decelerate various opportunities and national economic growth.

REFERENCES

[1] IEEE Standard 1159:Recommended Practice for Monitoring Quality Electric Power Quality,1995.

[2] IEEE Standard 519-1992: Recommended Practices and Requirements for HarmonicControl in Electrical Power Systems, IEEE, 1993.

[3] IEC 61000-4-30 77A/356/CDV, Power Quality Measurement Methods, 2001.

[4] SEMI Standard F-47: Semiconductor Equipment and Materials International, 1999.

[5] Information Technology Industry Council (ITI), 1250 Eye Street NW, Suite 200,Washington, D.C.

[6] Delfanti, M., Fumagalli, E.,Garrone, P., Grilli, L., Schiavo, L.L. (2010).Toward Voltage-Quality Regulation in Italy. *IEEE Transactions on Power Delivery*, 25(2), pp.1124-1132.

[7] The Norwegian directive on quality of supply, The Norwegian Water Resources and Energy Directorate, KarsteinBrekke, FrodeTrengereid and EspenLier, ISSN: 1501-2840.

[8] Sand, K., Seljeseth, H., Samdal, K. (2005). Power quality regulation in Norway. Electrical Power Quality and Utilization Magazine, 1(1), pp.45-49.

[9] Fayyaz, A. M.,Mumtaz, B. S. (2001). A sample power quality survey for emerging competitive electricity market in Pakistan.*In the Proceedingsof*IEEE International Conference on Technology for the 21st Century(INMIC 2001), pp. 38 – 44.

[10] Singh, L.P., Jain, S.P., Jain, D.K. (2009). Power quality related consumers rights in Indian electricity market. *In the Proceedingsof* IEEE International Conference on Electrical Power & Energy (EPEC), pp.1-6.

[11] Arrillaga, J., Bollen, M.H.J., Watson, N.R., (2000).Power quality following deregulation.*In the Proceedings of* the IEEE,88(2), pp. 246-261.

[12] Vannoy, D.B., McGranaghan, M.F., Halpin, S.M.; Moncrief, W.A., Sabin, D.D. (2007). Roadmap for power quality standards development, *IEEE Transactions on Industry Applications*, 43(2), pp.412-421.

[13] IEEE Standard 1346–1998: Recommended practice for evaluating electric power system compatibilitywith electronic process equipment.

[14] Kovel, D.O., Bocancea, R.A., Yao, K., Hughes, M.B. (1998). Canada national power quality survey: frequency and duration of voltage sags and surges at industrial sites," *IEEE Transaction on Industrial Application*, 35(5), pp. 2189-2196.

[15] Goldstein, M., Speranza, P.D. (1992). The quality of US commercial AC power supply," *In the Proceeding of*International Conference on IEEE INTELEC'92, pp.28-33.
[16] Douglas, J. (1993). Solving problems of power quality", *EPRI Journal*,18(8), pp.6-15.
[17] Lamedica,R., Esposito,G., Tironi,E., Zaninelli,D. Prudenzi,A. (2001). A survey on power quality cost in industrial customers.*In the Proceeding of*IEEE Power Engineering Society Winter Meeting, 2, pp. 938-943.
[18] Hunter,I. (2001). Power quality issues-a distribution company perspective.*IEE Power Engineering*, 15(2), pp. 75-80.
[19] _____Poor power quality costs European business more than €150 billion a year, Leonardo Energy 2008.
[20] Kocyigit,F., Yanikoglu,E., Yilmaz,A. S., Bayrak,M. (2009). Effects of power quality on manufacturing costs in textile industry. *Scientific Research and Essay*, 14(10), pp. 1085-1099.
[21] Rogers, B., Stephens, M., Magranaghan, M. F., (2004). Power quality issues and solutions in the automotive industry, *In the Proceeding of*International Conference on Power System Technology (POWERCON 2004), Singapore, pp. 238-243.
[22] Yin,S.A., Lu,C.N., Liu,E., Huang,Y.C., Huang,C.Y.(2001). A survey on high tech industry power quality requirements. *In the Proceeding of* Transmission and Distribution Conference and Exposition, 2001 IEEE/PES. 1. pp. 548-553.
[23] Muhamad, M.I., Mariun, N., Radzi, M.A.M. (2007). The effects of power quality to the industries, *In the proceeding of* the 5th Student Conference on Research and Development-SCORed 2007, Malaysia. pp.1-4.
[24] Vegunta, S. C.,Milaniovic, J.V. (2009). Financial impact of power quality on Indian pharmaceutical industry-survey results.*In the Proceeding of*20th International Conference and Exhibition on Electricity Distribution - Part 1, CIRED 2009. 2, pp.1 - 4.
[25] Chowdhury, B. (2001). Power quality.*IEEE Potentials*, 20, pp. 5–11.

A Techno-Economic Assessment of a Second Generation Biofuel Concept for Southern Thailand

Magnus Fröhling, Frederik Trippe, Kannokorn Hussaro, and Frank Schultmann

Abstract*— *Biomass valorization concepts such as second generation biofuels aim at decreasing the dependency on limited fossil resources and reducing climate relevant CO_2 emissions. Besides these aspects the elaboration of bio-economy concepts offers great economic potentials all along the value chain. Accordingly, numerous process chains are discussed and developed. Crucial factors regarding the economic feasibility of such concepts are the availability and costs of the feedstock, i.e. the biogenic raw material. It is one central task to ensure the provision of the necessary amounts and qualities of biogenic raw material at reasonable costs. South-East Asian and Latin American countries open new opportunities through often large amounts of so far unused biogenic raw materials. The aim of this contribution is to carry out a techno-economic assessment of one promising second generation biofuel concept for southern Thailand and compare it with findings of similar studies for Germany.

***Keywords*— Biomass-to-liquid fuel (BtL) production, palm kernel shells, techno-economic assessment, Thailand.**

1. INTRODUCTION

A large variety of valorization chains for biogenic raw materials is currently under discussion and development. Aim of these valorization chains is to substitute limited fossil resources and reduce the dependency on these, reduce fossil-based CO_2-emissions in order to meet the challenge to decrease the anthropogenic climate change and to open economic development possibilities. Crucial for the economic viability of such concepts is a secure supply of the necessary amount and quality of the feedstock material at reasonable cost. As they offer often large amounts of so far unused raw materials such concepts are widely discussed also for South-East-Asian and Latin American countries. Nevertheless, before detailed studies can be carried out, pilot or industrial scale plants have to be built. Promising concepts should be evaluated to prove the assumptions and identify key parameters for a successful implementation.

This study aims at carrying out such a first techno-economic assessment of one possible biomass valorization chain for biomass-to-liquid (BtL) fuel production, a second generation biofuel production via fast pyrolysis, gasification, gas cleaning and conditioning and Fischer-Tropsch synthesis. In the following section we describe our methodological approach. Afterwards we present the results and discuss these before we draw conclusions from our study.

Magnus Fröhling (corresponding author), Frederik Trippe and Frank Schultmann are with the Institute of Industrial Production at the Karlsruhe Institute of Technology (KIT), Hertzstraße 16, D-76187 Karlsruhe. Phone: +49 721 608 44400; Fax: +49 721 608 44682; E-mail: magnus.froehling@kit.edu.

Kannokorn Hussaro is with the Eastern-Asia University, Pathum Thani, Thailand.

2. METHODOLOGICAL APPROACH

Reference configuration of a BtL production chain

To carry out the techno-economic assessment we refer to a reference configuration of a BtL production chain in order to achieve results which are comparable to similar studies carried out e.g. for Germany (see e.g. **Error! Reference source not found.**, **Error! Reference source not found.**). In our reference configuration the biomass is dried and milled in order to achieve optimal conditions for the subsequent fast pyrolysis. The pyrolysis step is taken out in five decentralized plants with a capacity of about 100 MW thermal input. The produced intermediate – the so called slurry or biosyncrude – is gasified in an entrained-flow reactor under high pressure (40 bar) and high temperature (1,200 °C). Thus, a tar-free synthesis gas is produced. In order to fulfill the requirements of the FT synthesis, the gas is cleaned from its pollutants by using conventional low-temperature gas cleaning techniques, i.e. cyclone, bag filter and a wet scrubber. To reach optimal synthesis conditions a H_2/CO molar ratio of 2:1 is required. Therefore a CO conversion is installed. After the FT synthesis in a fixed bed reactor with cobalt as catalyst, the synthesis products are separated by distillation into wax, diesel and gasoline. The gained waxes are converted with a hydrocracker into diesel and gasoline, leading to an increased biofuel production. The described reference configuration is depicted in **Fig. 1**.

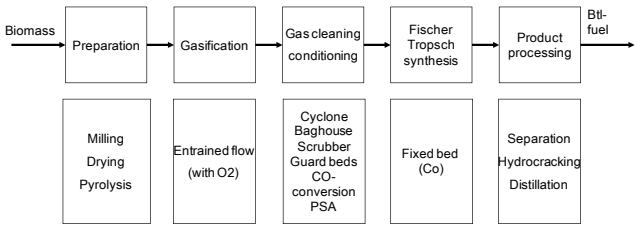

Fig. 1: Reference process chain.

Biomass potential analysis

Based on the requirements of this reference configuration a biomass potential analysis is carried out. Therefore biogenic residues in Thailand are investigated in terms of available amounts, locations of accruance, chemical characteristics and prices. Thus a suitable feedstock for the further studies is identified.

BtL production network design

On the basis of the reference configuration and the results from biomass potential analysis a BtL production network is elaborated. Sources for the feedstock, locations and structure of the fast pyrolysis and the gasification plants are determined as well as feedstock supply, transport distances and costs.

Material and energy balancing

For the described reference configuration a mass and energy flow balancing is carried out. For the first step, i.e. the pyrolysis plant a detailed analysis based on spreadsheet simulation is performed. The second processing step, i.e. gasification, is done using literature data. The further steps are balanced using the flowsheeting system Aspen Plus, which is capable to model thermodynamic reactions by the use of pre-defined reactor modules and comprehensive material data bases (cf. **Error! Reference source not found.**, **Error! Reference source not found.**). The results of this balancing are characteristic dimensions of the processing units such as reactor sizes, needed thermal power etc. and the material and energy input and output flows. These serve as a basis for the further economic assessment which is described in the following sections.

Economic assessment

The economic assessment aims for determining production costs of BtL fuel and to compare these with market prices for fossil based gasoline and diesel. Further the production cost of the intermediate, the so called slurry or biosyncrude is compared with the market prices for coal and gas which are the raw materials in coal-to-liquid (CtL) and gas-to-liquid (GtL) plants and which could be partly replaced by biosyncrude. To achieve this, the total capital investment (TCI) for several decentralized fast pyrolysis plants and the centralized gasification and synthesis plant has to be estimated at first. For this purpose, all main equipment components have to be designed according to the mass and energy flows and their investment data has to be gathered.

Investment data for the main equipment components are taken from Peters et al. **Error! Reference source not found.** for standardized components. For special components, vendor quotes from respective suppliers are taken into account. The values derived from literature data are scaled up or down using specific scaling factors for the components in order to reach the needed dimensions. Since the investment data provided by Peters et al. **Error! Reference source not found.** dates back to the year 2002, they have to be updated to 2008. To do so, the average Chemical Engineering Plant Cost Index for the year 2008 is used. Finally the investment data are converted from US$ to € using the yearly average exchange rate of 1.483 US$ per € in 2008.

Based on the investment data for the main equipment components, the total capital investment can be estimated using ratio factors for direct and indirect capital investment for each component. Differentiated additional charges Z_i (“overall installation factors”) are added to consider additional direct (instrumentation and control, buildings, grid connections, site preparation, civil works, electronics and piping) and indirect costs (engineering, building interest, project contingency, fees, overheads, profits, start-up costs). Thus, the total capital investment is estimated according to equation 1. As the direct costs decrease with increasing capacities, the factor A_i for the direct costs is scaled in dependency on the component capacity P_i in comparison to a basic capacity P_{basis} with a factor of -0.82. Where no differentiated factors are available a factor of 1.995 is used for Z_i, comprising a factor of A_i = 0.33 for the direct and a factor of 0.5 for the indirect costs B_i. The equations 1-3 show the described relationships.

$$Total\,Capital\,Investment\,(TCI) = I_{ME} \cdot \sum_{i=1}^{m} Z_i \qquad (1)$$

I_{ME} *Investment for main equipment components*

Z_i *Factor for direct/indirect capital investment*
i = 1...m

$$Z_i = (1 + A_i) \cdot (1 + B) \qquad (2)$$

$$A_i = 0.33 \cdot \left(\frac{P_i}{P_{basis}} \right)^{-0.82} \qquad (3)$$

The factors are adapted to process conditions, design complexity and required materials of the BtL facilities considered in this study. The applied factor method implies uncertainties of plus/minus 20.

After estimating the total capital investment, annual production costs can be derived. The annual production costs consist of investment dependent, personnel and consumption dependent costs. The investment dependent costs in turn are comprised of capital costs, maintenance as well as taxes and insurance. Biomass feedstock and transportation, slag disposal, electricity and cooling water make up the consumption dependent costs. Finally the costs for producing BtL fuels are reduced by the revenues from selling excess electricity to the grid. The composition of the annual production costs is summarized by Equation 4.

$$\begin{aligned} C_{Produtcion} = {} & TCI \cdot (p_a + p_m + p_t + p_i) + C_{Personnel} \\ & + C_{Biomass} + C_{Electricity} + C_{Cooling\ Water} \\ & + C_{Slag} - R_{Electricity} \end{aligned} \qquad (4)$$

p_a *Annuity factor*

p_m *Percentage of TCI for maintenance*

p_t *Percentage of TCI for taxes*

p_i *Percentage of TCI for insurance*

The annuity method translates the initial investment, which is assumed to be the TCI estimated before, into a stream of identical payments for a given number of years. These identical payments represent interests on and depreciation of the capital investment. The annuity factor is calculated according to Equation 5 and states a percentage of TCI.

$$p_a = \frac{(1+i)^n \cdot i}{(1+i)^n - 1} \quad (5)$$

i *Interest rate*

n *Expected lifetime*

The parameters used in this study to calculate the production cost of BtL fuel in Thailand are an interest rate of 5.875% p.a. and 20 years expected lifetime. The interest rate is believed to be the average rate over the 20 years time span in Thailand. The recovery value of the BtL production facilities after the expected lifetime of 20 years is assumed to equal zero.

The average annual maintenance costs for the pyrolysis plant and the gasification and synthesis plant equal about 4% of the BtL facilities' TCI per year.

Finally it is assumed, that insurance and taxes contribute with annually 1% of TCI each to the annual production costs of the biosyncrude.

The personnel demand and costs estimation is based on average data for workforce in Thailand. Personnel costs equal on average about 10,000 € per employee and year. The overall number of personnel needed in three shift operation sums up to 46 employees.

Costs for consumption dependent material flows depend on plant availability. On average 7,000 operating hours per year are assumed in the five pyrolysis plants and 7,500 operating hours in the gasification and synthesis plant, which correspond to about 80% and 85%, respectively, plant availability during the expected lifetime. The price of electricity equals the average in Thailand of 49.30 €/MWh. The excess electricity in the gasification and synthesis plant is assumed to be sold at the same price to the existing grid. Cooling water is assumed to be available at a price of 2 €/m^3 and the slag is considered to be disposed of at 30 €/t. Since the prices for biomass feedstock, electricity and cooling water will vary during the considered life time, these prices should be regarded as average values.

3. RESULTS

Biomass potentials

To avoid conflicts with the food or other established agricultural chains we focus on a number of promising biogenic residues. Thailand has a potential of so far unused biogenic residues of more than 30 m t **Error! Reference source not found.**. Besides cassava rhizomes, rice straw, which is mainly burned on the fields, and corn straw especially residues from sugarcane, rice and palm oil production come into focus. They accrue in orders of magnitude which are interesting for an industrial scale BtL plant. Contrary to e.g. rice and corn straw they accrue in processing plants and therefore have no or only very small costs of capture. Further, the lower heating values (LHV) for sugarcane trash, rice husk and especially palm kernel shells make them interesting for further investigations (see Table 1).

Table 1: Biomass potentials in Thailand (2008)

Biomass	Produc-tion [10^6 t]	Biomass residues	Residues [10^6 t]	LHV [kJ/kg]
Sugarcane	73.5	Sugarcane trash	21.315	15.479
Rice	31.47	Rice husk	6.923	14.204
Palm oil	9	Palm kernel shells	1.71	16.900
		Empty fruit bunch	2.07	7.240

Source: [5]

Looking at the chemical analysis of the named promising biogenic residues shows, that especially palm oil shells are well suited as they have acceptable moisture content, the highest amount of carbon combined with the lowest or very low ash, chlorine and sulfur contents (see Table 2).

Table 2: Analysis of the selected biomass residues

Composition	Sugarcane trash [%]	Rice husk [%]	Palm oil shell [%]
Moisture	9.2	8.2	12
Fixed-C	18.61	21.46	18.5
Volatile	74.67	64.16	77.5
Ash	6.72	14.38	4
C	45.82	42.59	50.52
H	5.59	4.89	5.69
O	41.22	37.8	39.43
N	0.45	0.2	0.32
Cl	0.01	0.1	0.02
S	0.2	0.04	0.02

Source: [4]

Further the geographical location of the accruance of the palm kernel shells is favorable in comparison to the other biomass types. Currently there are somewhat more than 50 palm oil mills located in the southern part of the

country. These are spread about seven provinces. The biomass potentials in these seven provinces are given in Table 3. The palm oil mills in southern Thailand supply combined an amount of nearly 850,000 t per year on a dry basis. This amount is sufficient to provide the feedstock for an industrial scale realization of the BtL plant.

Therefore palm kernel shells are selected as the most promising biomass type for the further considerations of this study. It is assumed that with an average price of 26 €/t on a dry basis the necessary amount of feedstock can be secured. The price includes the transportation from the palm oil mill to a collection point or the pyrolysis plant within the province.

Table 3: Palm kernel shell accruance in southern Thailand

Province	Amount of Palm oil shells [t/a]
Surat Thani	253,499
Krabi	222,870
Chumphon	180,145
Trang	101,430
Songkhla (Hat yai)	44,988
Satun	34,500
Phangnga	2,243
Total	839,675

Source: [5]

BtL production network design

Taking into account the transport distances by rail and truck (see Table 4) and the corresponding transportation costs for biomass from the collection point to a pyrolysis plant and for the slurry from the pyrolysis plants to the gasification plant a BtL production network is elaborated.

Table 4: Transport distances between the provinces in southern Thailand

Transport distances	*Distance (rail) [km]*	*Distance (truck) [km]*
Chumphon – Surat Thani	117	197
Krabi – Surat Thani	-	211
Trang – Surat Thani	220	226
Phangnga – Krabi	-	86
Satun – Trang	140	140
Songkhla (Hat yai) – Trang	-	148

This network comprises five fast pyrolysis plants in four locations (Chumphon, 2x Surat Thani, Krabi and Thrang) and one central 500 MW gasification and synthesis plant located in Surat Thani). The needed biomass for the fast pyrolysis plants is supplied by these regions, to utilize the built capacities the available amounts from Phangnga are delivered to Krabi and from Satun and Songkhla to Trang. The production network is given in **Fig. 2**. This BtL production network serves as a basis for the further calculations.

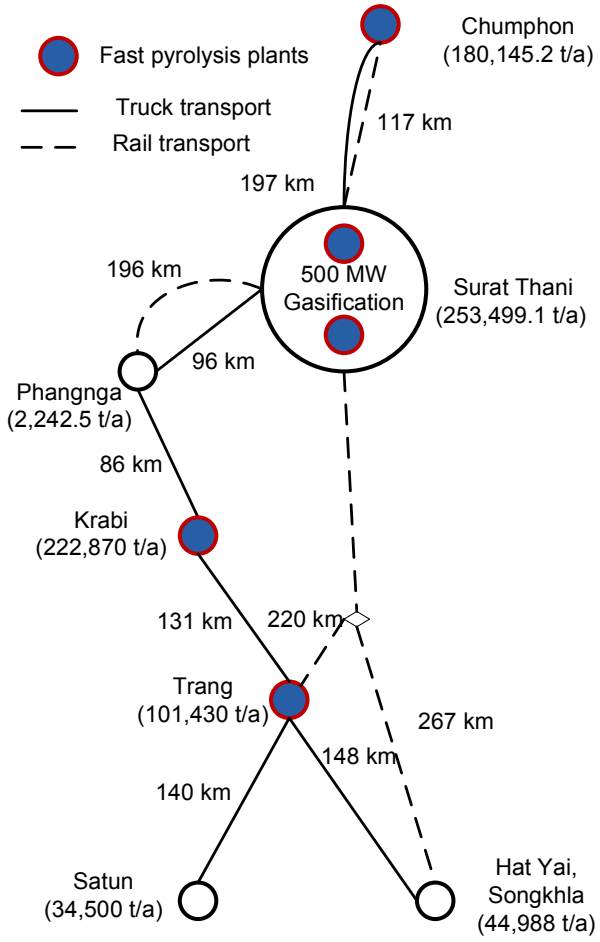

Fig. 2. BtL production network.

Resulting material and energy flows

The mass and energy flow balancing leads to an estimated production of approximately 120,000 t of fuel and a generation of excess electrical power of about 5.5 MW_{el} in the centralized gasification and synthesis plant. This output is met by setting up the network of five decentralized pyrolysis plant with each about 100 MW thermal input capacity. With a lower heating value of about 14 MJ per kg palm oil residues on a wet basis, a single pyrolysis consumes on average 25 t of biomass per hour. On a mass basis around 70% of the palm oil residues remain in the biosyncrude. The mass losses are mainly caused by drying and burning of pyrolysis gas which cannot be integrated into the biosyncrude and is therefore used to supply the thermal energy in the decentralized pyrolysis plants. On an energy basis 85% of the heating value remain in the biosyncrude, resulting in a higher heating value of about 18.5 MJ per kg biosyncrude. On a yearly basis the five decentralized pyrolysis plants deliver combined about 600,000 t Slurry

to the centralized gasification and synthesis plant. The gasification of the delivered slurry yields about 125,000 t per year of raw synthesis gas. The entrained flow gasification is performed at high pressure (40 bar) and high temperature (1,200 °C) in order to avoid the building of tar. Pure Oxygen is used as gasification agent. Maintaining the high gasification temperature requires a relatively high amount of oxygen. On a yearly basis around 300,000 t oxygen are needed which corresponds to a lambda value of about 0.4. After cleaning the raw synthesis gas, the Fischer-Tropsch synthesis produces about 120,000 t of BtL fuel per year from the cleaned and conditioned synthesis gas, i.e. carbon monoxide and hydrogen. An overview of the resulting mass flows is given in **Fig. 3**.

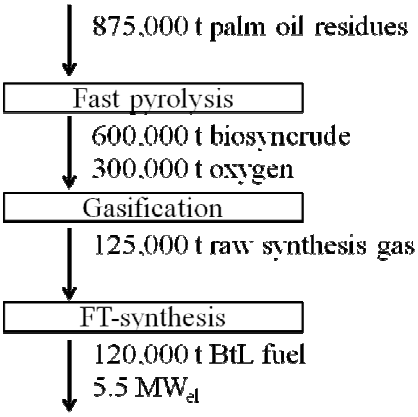

Fig. 3. Resulting main mass and energy flows for the considered process chain on a yearly basis

Economic results

The aim of the economic assessment is twofold. The most interesting problem to be solved is determining the production costs of BtL fuel and to compare these with market prices for fossil based gasoline and Diesel. Previous studies revealed that producing BtL fuels in Europe or the US is highly capital intensive. Total capital investment needed to build a complete network of pyrolysis and gasification and synthesis plant is most likely to excess the amount of 1 billion €. This in turn leads to the assumption that the starting point for setting up a BtL facility network could be a first pyrolysis plant. Therefore the production cost of the intermediate slurry biosyncrude is compared to the market prices for coal and gas which are the raw materials in CtL and GtL plants and which could be partly replaced by biosyncrude.

Another aspect is to estimate the competitive advantage of South-East Asian countries, such as Thailand for biofuel production due to their relatively low prices for biogenic resources. This effect can be demonstrated impressively at the production cost of the intermediate biosyncrude.

To build a pyrolysis plant with an thermal input capacity capacity of about 100 MW would require a total capital investment of about 40 million €. Summing up the constituents of production costs on an annual basis and dividing it by the annual slurry production on a HHV basis leads to the specific production costs of the biosyncrude. With the assumed annual operation time of 7,000 hours the pyrolysis plant is able to produce approximately 617,000 MWh biosyncrude or slurry on a HHV basis.

Fig. 4 states the production costs per MWh biosyncrude in comparison with the market prices for oil and gas in Thailand. To demonstrate the regional advantage of Thailand the production cost for Germany are presented as well.

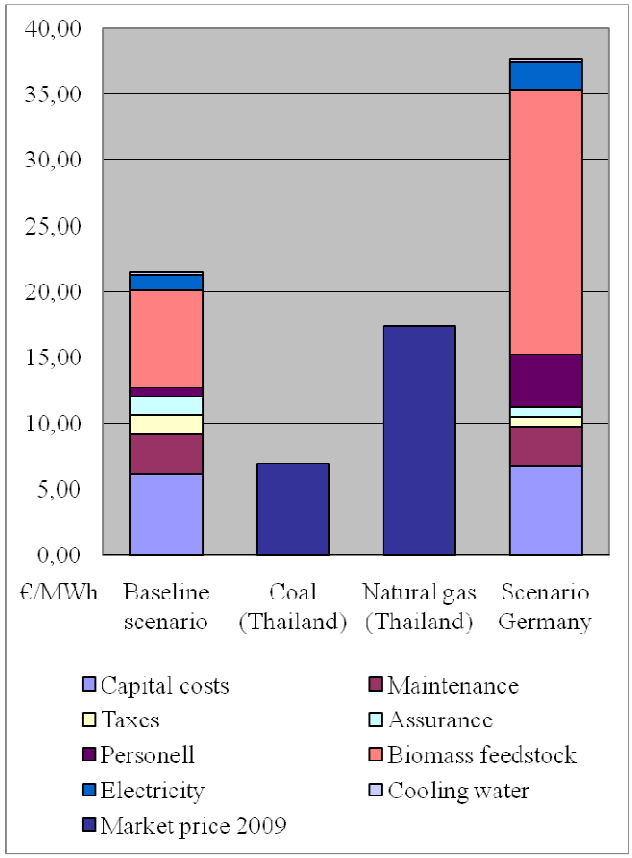

Fig. 4. Production costs of slurry

As indicated by the baseline scenario in the

Fig. 4, investment dependent costs make up a 57% share, personnel a 3% share and consumption dependent costs a 40% share of production costs. Within the consumption dependent costs the biomass feedstock is the most important contributor which amounts to about 34% of total production costs. The slurry can be produced at costs of about 22 €/MWh in Thailand.

An indicator for the competitiveness of biosyncrude compared to other resources for XtL-technologies is the comparison of the biosyncrude production costs to coal and gas market prices. Obviously the biosyncrude is not competitive in Thailand at the moment.

But there are strategies to market biosyncrude from Thailand. For example via exporting biosyncrude to Germany where it is almost twice as expensive to

produce due to higher biomass feedstock prices as well as higher costs for workforce. A viable option for the realization of a BtL production network would be to place the pyrolysis plants in Thailand with relatively low capital investments and process the biosyncrude in the capital intensive gasification and synthesis plant in Europe.

Concerning the determination of the production costs for BtL fuels in Thailand the total capital investment for this network producing about 120,000 t of BtL fuel per year sums up to about 650 million €. The corresponding annual production cost divided by the annual production of BtL fuel result in the specific production cost per liter fuel. BtL fuel could be produced at costs of about 0.93 € per liter. This is above current market prices for gasoline and diesel which are currently about 0.70 €/l (see, e.g., **Error! Reference source not found.**). The composition of the BtL production costs is shown in **Fig. 5**.

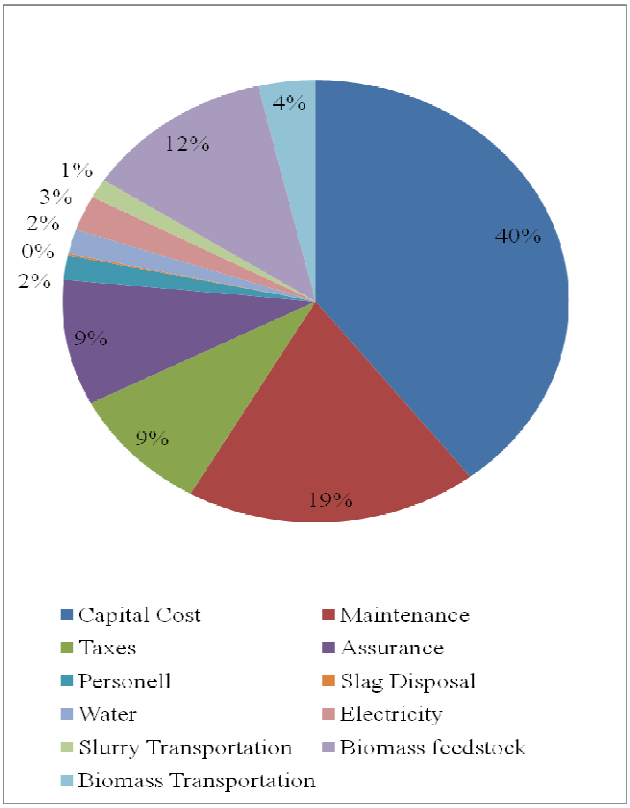

Fig. 5. Composition of production costs of BtL fuel.

The composition of these costs indicates the capital intensity of the BtL fuel production network. Implying the capital dependent costs cost from the slurry production, the share of capital dependent costs in the total production costs of BtL fuel amounts to about three quarters. The slurry production and transportation to the gasification and synthesis plant contributes about 47% to the production costs of the final BtL fuel.

4. SUMMARY AND CONCLUSIONS

In this contribution a first techno-economic assessment of a potential BtL concept is made for Thailand. Based on a biomass potential analysis a BtL production network is elaborated and economically assessed.

A possible BtL production in Thailand can be located in the southern part of the country. A promising feedstock in terms of location of accruance, amounts, chemical characterization and price are palm kernel shells which can be collected from the about 50 palm oil mills in southern Thailand. They are estimated to be provided to a collection point or a pyrolysis plant in each of the seven considered provinces at about 26 €/t on a dry basis.

The economic assessment of the BtL production shows that additional development efforts are needed in order to make the process chain profitable. The production of the intermediate slurry or biosyncrude shows lower costs per MWh in comparison to estimations for Germany. Nevertheless these costs are still higher than those of comparable fuels for XtL technologies, i.e. coal and natural gas. As the slurry/biosyncrude has a volumetric energy density comparable to crude oil they are economically shippable and international market potentials exist in a export e.g. to European countries.
Starting point for further developments is the capital intensity of the BtL production chain. Both, for the production of slurry/biosyncrude via fast pyrolysis and diesel via the whole process chain investment dependent cost make up the most important parts of the annual costs (57% and 77%). When one succeeds in reductions here and/or crude oil prices rise without affecting the prices for the biogenic residues the gap to profitability may be closed.

REFERENCES

[1] Chongkum, W. (2007). Connecting Knowledge, presentation at the Thai-German Colloquium on Sustainable Use of Biomass, Karlsruhe, 11/16/2007.

[2] Fröhling, M. (2006). Zur taktisch-operativen Planung stoffstrombasierter Produktionssysteme, Deutscher-Universitätsverlag, Wiesbaden.

[3] Kerdoncuff, P. (2008). Modellierung und Bewertung von Prozessketten zur Herstellung von Biokraftstoffen der zweiten Generation, Universitätsverlag Karlsruhe, Karlsruhe.

[4] Laohalidanond, P and Wirtgen, C. (2007) The potential of biomass in Thailand and the production of synthetic diesel fuel from Thai biomass, 15th European Biomass Conference & Exhibition, 7-11 Mai 2007, Berlin.

[5] OAE (2009) Data obtained from the Office of Agricultural Economics Thailand.

[6] Peters, M.S., Timmerhaus, K.D. and West, R.E. (2004) Plant Design and Economics for Chemical Engineerss, Mc Graw Hill, New York.

[7] Shell, (2010), Fuel prices. Homepage of Shell Thailand, URL: http://www.shell.co.th/, retrieved September 2010.

[8] Trippe, F., Fröhling, M., Schultmann, F., Stahl, R., Henrich, E. (2010). Techno-economic analysis of fast pyrolysis as process step within a biomass-to-liquid (BtL) fuel production. In: *Waste and Biomass Valorization* 1 (4): 415-430.

Bio-Gasoline Production from Bio-Diesel via Catalytic Cracking Reaction on Platinum Zeolite Catalyst

Nantawat Usomboon, Malee Santikunaporn, and Suchada Butnar

***Abstract*— *The catalytic cracking of bio-diesel has been investigated in a continuous fixed bed reactor over Pt/zeolites. Three different zeolites (Y, BETA and MOR) were used as supports impregnated with 1 wt% of platinum metal. The reacations were carried out in hydrogen flow under the following conditions, the temperature range of 573 K - 653 K, and WHSV of 22.9-43.7 h^{-1}. The results showed that these composite catalysts have the potential to be used in bio-gasoline production. At 613 K, the Pt/MOR showed complete conversion of bio-diesel to cracking products. The Pt/Y showed not only high conversion, but also high selectivity to bio-gasoline when compared to Pt/BETA. In addition, the conversions were strongly dependent on both temperature and WHSV.*

***Keywords*— Composite catalyst; bio-diesel; catalytic cracking.**

1. INTRODUCTION

The rapid increase of energy consumption and the environmental concerns have made biofuels gain more attention over last decade. Biofuel or blend of biofuels can be substituted for regular fuel in all vehicle types. In addition, it has been literally reported that the performance and combustion of bio-fuels are as good as regular fuels [1].

Bio-gasoline, one of alternative fuels used in gasoline engines, is hydrocarbon biofuel produced from biomass. While much attention has been given to the use of biomass to produce ethanol, methods are currently being developed for producing hydrocarbon fuel from biomass. This is because the hydrocarbon biofuels are energy equivalent to and chemically the same as petroleum-based fuels. Many novel pathways to produce bio-gasonline have been studied. However, it is literally reported that catalytic cracking process would be the potential route to provide clean fuel [2-4]. The catalytic cracking process shows several clear advantages in comparison with pyrolysis, fermentation and transesterification processes. The reaction temperature for the catalytic cracking process is lower than pyrolysis. The production of ethanol via fermentation requires a necessary pretreatment of feedstock with processes such as saccharification and hydrolysis. In addition, fermentation requires a much longer reaction time than the catalytic cracking process. Transesterification is only applied to the production of biodiesel whereas catalytic cracking can be applied for the production of kerosene, gasoline and diesel [4-5].

The key factor for the catalytic cracking reaction is the choice of catalysts. It is well-known that zeolites show excellent efficiency on catalytic cracking reactions. The important property of zeolites is the shape selectivity that controls product distribution in the process. Activity and selectivity of zeolites are managed by several factors such as acidity, pore size, pore distribution and pore shape. It is reported that cracking activity decreases with decreasing acidity [3,6]. For the catalytic cracking of palm oil on the composite zeolites, the maximum yield of gasoline and conversion obtained on REY composited with HZSM-5 showed 95.9 wt% conversion and 40.9 wt% gasoline yield due to high acidity [6]. For the meso-porous material MCM-41 and SBA-15, the similar results were obtained [7-8]. The effect of acidity on activity has been confirmed by Junming et al. [9]. The main products from the catalytic cracking over basic catalysts were liquid hydrocarbons in diesel range. As for the effect of pore size on selectivity, the smaller pore size provided the shorter chain of products [10].

The aim of the present work is to study the effect of bifunctional catalysts (Pt/HY, Pt/beta and Pt/MOR) on the conversion and selectivity to hydrocarbon products in gasoline range.

2. EXPERIMENTAL SECTION

2.1. FEED

Feed was the mixture of straight chain hydrocarbons containing carbon atoms in range of C15-C18 produced from the hydrodeoxygenation of palm oil. It can be referred to Bio-diesel. The distribution of compounds is reported in Table 1.

2.2. Catalysts

Bifunctional catalysts used in the catalytic cracking of bio-diesel were platinum supported on different zeolites (Y, beta and MOR). All zeolites were supplied from Zeolyst International Corp., USA. The properties of each zeolite are presented in Table 2.

Nantawat Usomboon and Malee Santikunaporn (corresponding author) are with Department of Chemical Engineering, Faculty of Engineering, Thammasat University, Patumthani 12120, Thailand. Email: smalee@engr.tu.ac.th.

Suchada Butnart is with Research and Technology Institute Research and Technology Institute, PTT Public Company Limited.

Table.1 Feed conposition

Component	Chemical structure	wt%	Total (%wt.)
Gasoline (C7-C10)	Straight chain	-	-
	Branched chain	-	
Kerosene (C11-C14)	Straight chain	1.1	1.1
	Branched chain	-	
Diesel (C15-C18)	Straight chain	98.7	98.8
	Branched chain	0.1	

Table 2 Zeolite properties

Properties	Y	BETA	MOR
Pore size (nm)	0.8	0.56 x 0.74	0.4
Surface area (m^2/g)	730	710	500
Si/Al ratio	5.1	38	4-12

2.3 Catalyst Preparation

Catalysts were prepared by an impregnation technique with 0.1 wt% of platinum metal. The precursor was tetraammineplatinum(II) nitrate ($Pt(NH_3)_4(NO_3)_2$, 99.995% metals basis) obtained from Aldrich Corp. After the impregnation, catalysts were dried at 393 K for 12 h and then calcined in air at 773 K for 6 h.

2.4 Activity Test

The cracking reaction of bio-diesel was performed over Pt/zeolites at 2.76 kPa, 22.9 h^{-1} and 573-653K. Fig. 1 shows the experimental setup for the catalytic cracking reaction. The catalyst was in a powder form in order to avoid mass transfer effect. In each run, the desired amount of catalyst was packed in the middle of reactor between quartz wool. The ceramic balls were placed above and below the catalyst bed. Before testing, catalyst was reduced under hydrogen flow at 723 K for 4 h. Subsequently, feed was injected by a syringe pump at the desired rate into the reactor. The temperature was monitored by a thermocouple positioned at the center of the catalyst bed. Hydrogen was used as a carier gas when the reaction takes place. The products then were cooled in a cooler. The condensed liquid was collected and analyzed by a gas chromatography equipped with a FID detector.

2.5 Product Analysis

Organic liquid products (OLP) were analyzed and categorized into 3 types based on molecular sizes and boiling temperatures: gasoline fraction (C7-C10), kerosene fraction (C11-C14) and diesel fraction (C15-C18). The standard properties are shown in Table 3.

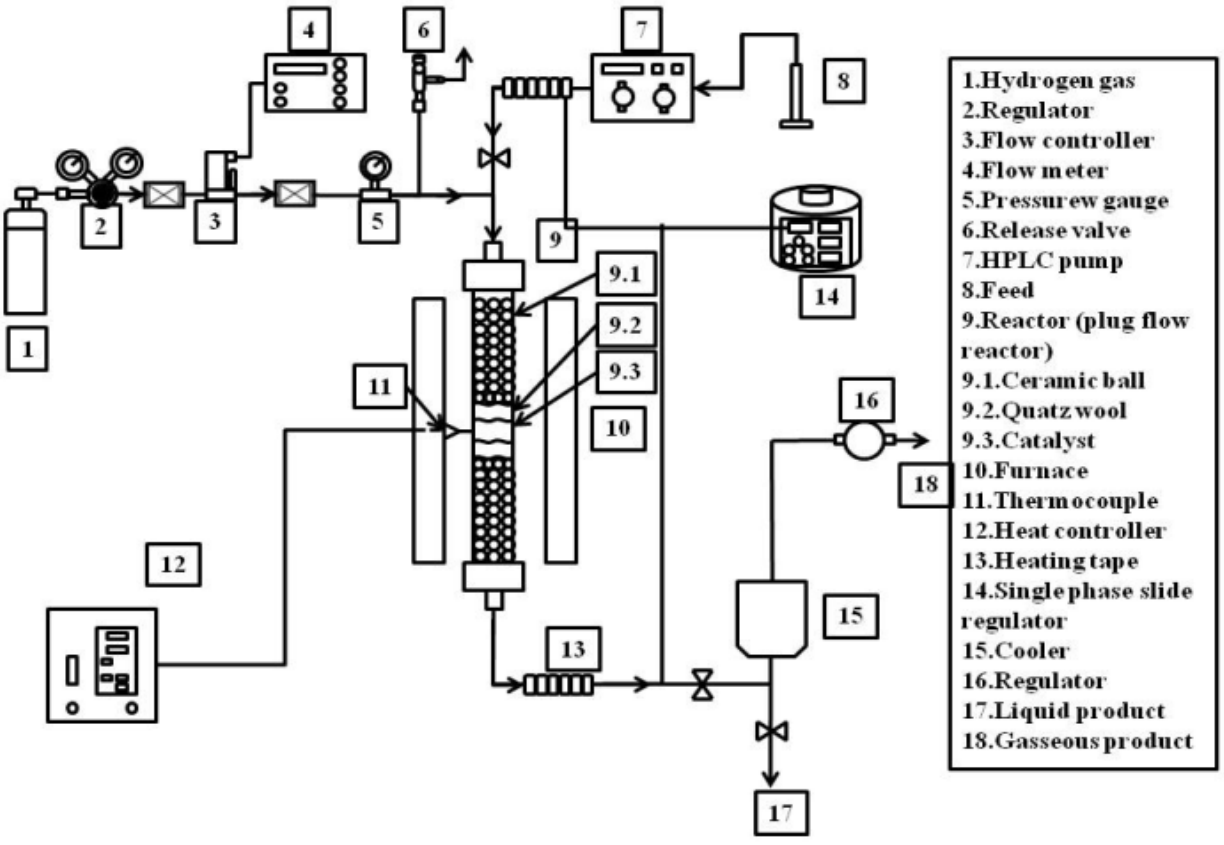

Fig. 1 Schematic reaction.

Table 3 Fuel standard

Property	Gasoline[(a)]	Kerosene[(b)]	Diesel[(a)]
Chemical formula	C4 - C12	C8 - C16	C8 - C25
Boiling point (K)	299.66 - 528	392 - 573	453 - 613
Freezing point (K)	-40	Below 233	233 - 243
Auto ignition temp. (K)	530.22	No report	~588.66
Flash point (K)	230.22	311	333 - 353
Density (kg/m^3 at 288 K)	718.96 – 778.87	775 - 840	848.25
Viscosity at 253 K (mm^2/s)	0.8 – 1.0	8	9.0 – 24.0
Octane no. (RON/MON)	88 – 98/80 - 88	-	-
Cetane no.	-	-	40 - 55
Lower heating value (kJ/m^3)	32.3x10^6	n/a	35.8x10^6
Higher heating value (kJ/m^3)	34.6x10^6	n/a	38.3x10^6

a.United state department of energy, www.Energy.gov.

b.Fuel properties – effect on aircraft and infrastructure, Aviation rulemaking advisory committee.

Table 4. Composition of liquid products obtained from the catalytic cracking reaction over various Pt/zeolites. Reaction condition: Temperature 613 K, Pressure 2.76 kPa and WHSV 22.9 h^{-1}.

		Feed	Catalyst		
			Pt/Y	Pt/BETA	Pt/MOR
Conversion (%)		-	78.6	33.4	100
Gasoline (C7-C10)	Straight chain	-	16.9	11.8	57.3
	Branched chain	-	28.5	17.6	42.7
	total	-	45.4	29.4	100
Kerosene (C11-C14)	Straight chain	1.1	3.9	2.1	-
	Branched chain	-	11.9	1.4	-
	total	1.1	15.8	3.5	-
Diesel (C15-C18)	Straight chain	98.7	21.2	65.8	-
	Branched chain	0.1	17.7	1.3	-
	total	98.8	38.9	67.1	-

The catalytic performance was measured in terms of conversion, yield and selectivity to products. The conversion and selectivity are defined as follows:

$$conversion\ (\%) = \frac{feed - OLP}{feed} \times 100 \quad (1)$$

$$selectivity\ to\ A\ (\%) = \frac{product\ A}{conversion} \times 100 \quad (2)$$

3. RESULTS AND DISCUSSION

The catalytic performance of three different catalysts was studied in terms of conversion and selectivity to products in gasoline fractions. It is known that the quality of gasoline is evaluated based on its octange rating which denotes the percentage by volume of branched-chain in the combustible mixture. In this present work, to investigate on the quality of bio-gasoline, the chemical composition of products in gasoline range was analyzed and classified, according to their molecular structures, into straight-chain and branched-chain hydrocarbons.

Table 4 shows the chemical compositions of feedstock and liquid products obtained from catalytic cracking reactions over Pt/Y, Pt/beta and Pt/MOR under the same reaction condition (2.76 kPa, 613 K and WHSV 22.9 h^{-1}). It was noticed that the Pt/MOR gave the complete conversion and the feedstock was completely converted into gasoline fractions. The Pt/Y gave a higher conversion than the Pt/beta about 2 times. This may be due to their characteristics such as pore size and acidity. As illustraed in Table 2, it is suggested that the pore size of Pt/MOR is the smallest, followed by Pt/BETA and Pt/Y whereas Pt/Y contains a higher acidity than Pt/beta.

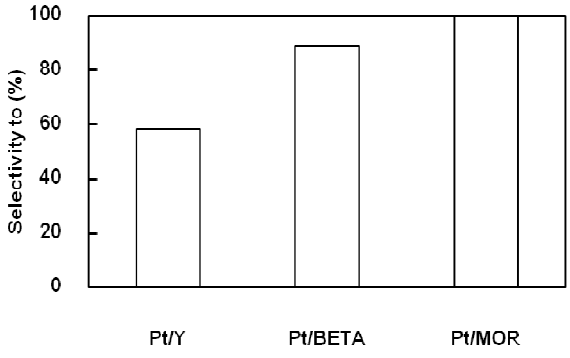

(a) Selectivity to gasoline fractions.

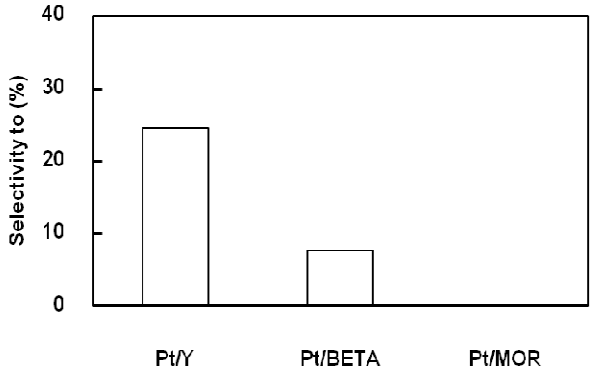

(b) Selectivity to kerosene fractions.

Fig. 2 Selectivity to gasoline and kerosene fractions over various catalysts. Reaction conditions: T = 613 K, P = 2.76 kPa, and WHSV = 22.9 h^{-1}.

Fig. 2 represents the selectivities to gasoline and kerosene fractions. It is evident that the highest selectivity to gasoline fraction was obtained when the cracking reaction were tested over Pt/MOR. In contrast, the highest selectivity to kerosene fraction was obtained when the Pt/Y catalyst was used. As mentioned above, the branched-chain structure are preferred to the straight-chain structure due to its knock resistance charactersitic. The ratio of branched-chain hydrocarbons to straight-chain hydrocarbons (B/S ratio) therefore was analyzed and illustrated in Fig. 3. The B/S ratios of the reactions on Pt/MOR, Pt/BETA and Pt/Y catalysts were 0.74, 1.49 and 1.69 respectively. It is implied that the Pt/Y gave the highest yield of branched-chain hydrocarbons.

It is evident that the Pt/BETA and Pt/Y gave the high yield of branched-chain hydrocarbons according to their B/S ratio. Therefore, the catalytic cracking reactions over both catalysts were further studied. To investigate the effect of reaction temperature on the product distribution, the reactions were conducted in a temperature range of 573 K to 653 K. Fig. 4 shows the comparison between the conversions obtained from catalytic cracking on Pt/Y and Pt/BETA. In the presence of both catalysts, the conversion of bio-diesel increases with increasing reaction temperature. It is however obvious that the conversion on the Pt/Y catalyst was higher than that on the Pt/BETA.

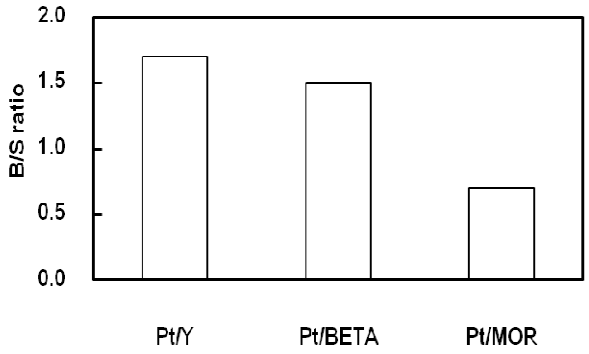

Fig. 3 The ratio of branched chain hydrocarbons to straight chain hydrocarbons in the gasoline fraction at 613 K.

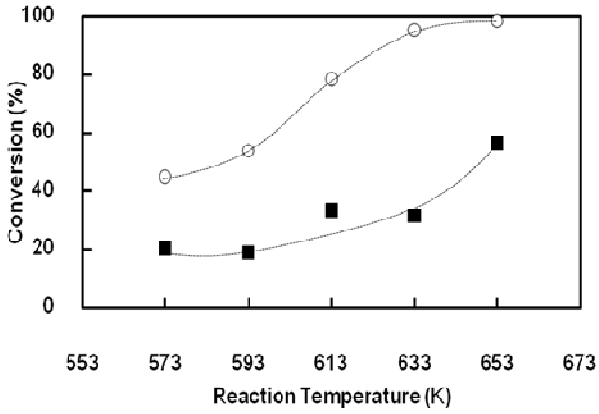

Fig. 4 Conversion obtained from catalytic cracking over Pt/Y and Pt/BETA as a function of temperature. Symbols: (○) for Pt/Y and (■) for Pt/BETA.

Fig 5 shows the effect of reaction temperature on the selectivity and B/S ratio of the cracking reactions. Interestingly, the reactions on both catalysts showed high selectivities to gasoline whereas the B/S ratios were not signifantly dependent on temperature reaction. It therefore may be concluded that the products obtained from the reactions on both catalyst would have the similar octane rating.

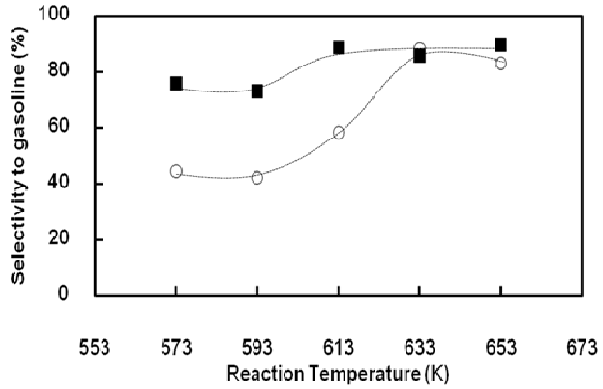

(a) Selectivity to gasoline fraction.

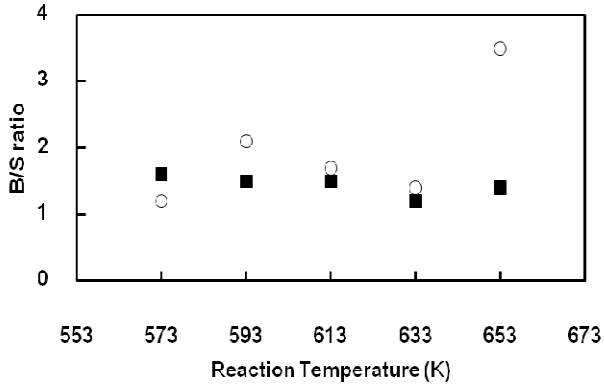

(b) The ratio of branched chain to straight chain hydrocarbon.

Fig. 5 Comparison of selectivity and ratio of branched chain to straight chain hydrocarbon over Pt/Y and Pt/BETA. Reaction conditions: T = 573-653 K, P = 2.76 kPa, and WHSV = 22.9 h^{-1}. Symbols: (○) for Pt/Y and (■) for Pt/BETA.

Finally, focusing on the catalytic activity of Pt/Y, the effect of space velocity were studied The catalyst reactions were conducted in a space velocity range of 23.3 – 43.5 h^{-1}. The conversion and selectivity to gasoline fraction were illustrated in Fig.6. It is evident that the conversion of bio-diesel decreases with increasing WHSV. However, the selectivity to gasoline fraction was independent of the WHSV.

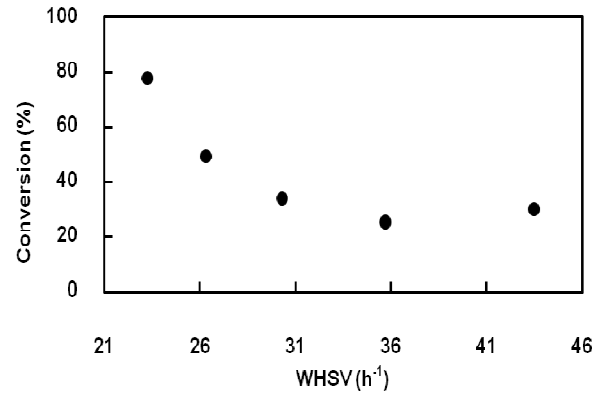

(a) Conversion

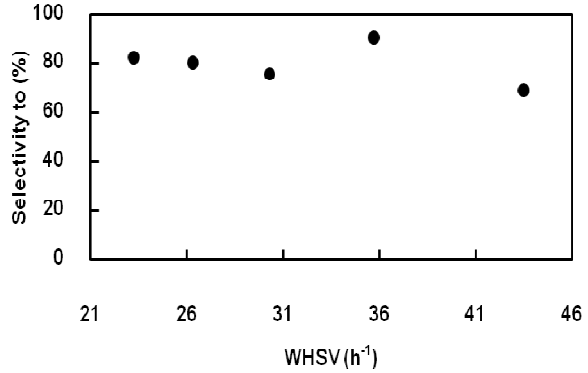

(b) Selectivity to gasoline fraction

Fig. 6 Conversion and selectivity to gasoline fraction over Pt/Y catalyst. Reaction condition: T = 613 K, P = 2.76 kPa, and WHSV = 23.3 – 43.7 h^{-1}.

4. CONCLUSION

Bio-gasoline produced from catalytic cracking of bio-diesel was studied over three different zeolites in the continuous packed bed reactor in a temperature range of 573-653 K. Among the three catalysts Pt/MOR showed the highest conversion and yield of gasoline fraction but the lowest B/S ratio. Both Pt/Y and Pt/BETA showed more suitable for this aspect. However, under the studied reaction conditions, the Pt/Y was the most efficient catalyst due to its high conversion and high selectivity to gasoline fraction compared to Pt/BETA.

ACKNOWLEDGEMENTS

The authors thank PTT Public Company Limited for financial support. The Faculty of Engineering, Thammasat University is gratefully acknowledged.

REFERENCES

[1] Adrian Zhou, Elspeth Thomson 2009. The development of biofuels in Asia. *Applied Energy* , s11-s20.

[2] Dr.SamaiJai-In. (n.d.). *BiofuelPrograms in Thailand : A Solution for Energy Sufficiency and Poverty Eradication?* URL www.mtec.or.th Access on 14/11/2010

[3] Yee Kang Ong, Subhash Bhatia (2010). The current status and perspectives of biofuel production via catalytic cracking of edible and non-edible oils. *Energy* , 111–119.

[4] Chew T.L and Bhatia S. 2008. Catalytic processes towards the production of biofuels in a palm oil and oil palm biomass-based biorefinery. *Bioresource Technology*, 99(17):7911–22.

[5] Klass DL. (1998). Biomass for renewable energy, fuels, and chemicals. San Diego, *CA: Academic Press.*

[6] Bhatia, S. 1999. Catalytic Conversion of Palm Oil to Hydrocarbons: Performance of Various Zeolite Catalysts. *Ind. Eng. Chem. Res.*, 3230-3237.

[7] Farouq A.A. Twaiq, A. M. (2004). Performance of composite catalysts in palm oil cracking for the production of liquid fuels and chemicals. *Fuel Processing Technology* , 1283– 1300.
[8] Bhatia, S. (2003). Catalytic conversion of palm oil over mesoporous aluminosilicate MCM-41 for the production of liquid hydrocarbon fuels. *Fuel Processing Technology* , 105-120.
[9] Xu Junming, J. J. (2010). Biofuel production from catalytic cracking of woody oils. *Bioresource Technology* , 5586–5591.
[10] Yean-Sang Ooi, S. B. (2007). Aluminum-containing SBA-15 as cracking catalyst for the production of biofuel from waste used palm oil. *Microporous and Mesoporous Materials* , 310–317.

SF_6 Capacitive Voltage Divider

Cattareeya Suwanasri and Thanapong Suwanasri

Abstract— *This paper aims to develop a 100 kV capacitive voltage divider. The divider was separated into high voltage and low voltage parts. The high voltage part was constructed from capacitors connected in series in order to obtain the capacitance as of 114.285 pF. The low voltage part was constructed from capacitors connected in parallel to obtain the capacitance as of 0.12 μF. This capacitive voltage divider was filled with three gas insulation as air, N_2 and SF_6 for each test in order to select the suitable gas insulation. The test procedures were followed the standard IEC 60060 - 2 (1994). The test records showed that the performance of the developed capacitive divider is within the designed standard.*

Keywords— **Capacitive voltage divider, measuring instrument, sulfur hexafluoride (SF_6).gas insulation.**

1. INTRODUCTION

The voltage divider is a simple tool for measuring the high voltage by using two impedances connected in series. It is a very useful device for high voltage measurement in several circuit e.g. insulation testing. The voltage divider can be used with resistive, inductive, or capacitive circuit elements. It can also measure the AC, DC or high voltage impulse voltage sources. However, capacitive dividers can usually used to measure the AC voltage, whereas it is not suitable for the DC input voltage measurement because the DC voltage could not pass through the capacitors. Capacitive voltage divider as shown in Fig. 1 produces an output voltage (V_{out}) which is a fraction of its input voltage (V_{in}).

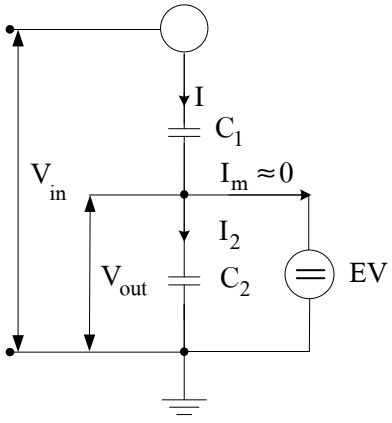

Fig. 1. Capacitive Voltage Divider [2]

where V_{in} = high voltage input (V)
V_{out} = low voltage output (V)
C_1 = high voltage capacitance (F)
C_2 = low voltage capacitance (F)
R_m = matching resistance (Ω)
EV = oscilloscope

Voltage division refers to the ratio of a voltage among the components of the divider. The 1000:1 is given in Eq. (1). The principle is that the current in series circuit is always equal. Therefore, the voltage ratio has C_1 in the numerator because of the inverse relationship between capacitive reactance and capacitance as shown in Eq. 1.

$$V_{out} = V_{in}\left[\frac{C_1}{C_1 + C_2}\right] \quad (1)$$

Since the voltage ratio of this capacitive voltage divider is opposite to resistive and inductive voltage divider, this should be carefully considered in output voltage calculation in order to avoid the mistake.

2. DESIGN AND CONSTRUCTION

Capacitive voltage divider has a large numbers of variables. The specification is given in Table 1. It is designed to meet the requirement of standard IEC 60060 - 2 (1994) [1]. The unit consists of two capacitors connected in series. The important components will be discussed.

Cattareeya Suwanasri (D.Eng) (Thailand (corresponding author) is working for the Department of Electrical and Computer Engineering, Faculty of Engineering, Naresuan University, Phitsanulok 65000. Phone: +66-5-596-4342; Fax: +66-5-596-4005; E-mail: cattareeyaa@nu.ac.th.

Thanapong Suwanasri (Asst. Prof. Dr.-Ing.) is working for the Sirindhorn International Thai-German Graduate School of Engineering, TGGS), King Mongkut's University of Technology North Bangkok, Bangkok 10800 Thailand. E-mail: thanapongs@kmutnb.ac.th.

Table 1. Specifications of Capacitive Voltage Divider

Parameter	Specification
Rated voltage	100 kV
High voltage capacitance	113.00 pF
Low voltage capacitance	0.108
Test voltage	110% of rated voltage (V)
Frequency	50 Hz
Scale factor	1000:1
Dielectric medium	SF_6, N_2, Air
Accuracy	±1%

2.1 Electrode length

The capacitors connected in series must be installed in the cylinder, which is made from Acrylic. To prevent the external flashover, the relative electrical clearance from top electrode to ground should be 5 m/MV (rms.) for AC voltage. Thus, the total length of 100kV divider should be at least 0.5 m. However to have some safety margin in operation, the length of cylinder in this design is one meter long**.**

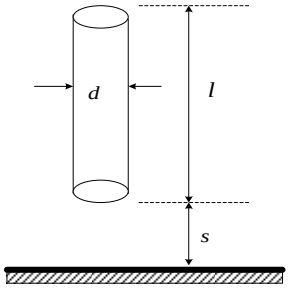

Fig. 2. Capacitor Cylinder

2.2 Stray capacitance

The unavoidable stray capacitors always occur between the divider and earth or the divider and grounded objects. A existence of stray capacitance can directly affect the measurement precision. Therefore, it should be investigated.

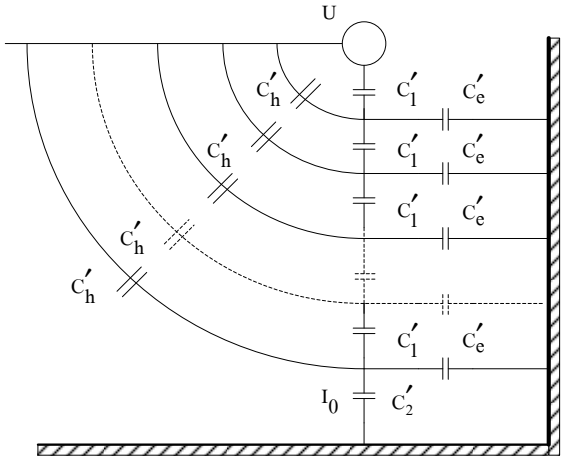

Fig. 3. Diagram of Measurement System

Fig. 3 shows the equivalent circuit diagram of measurement system that considered stray capacitance $C_e^{'}$ (pF), which is calculated as:

$$C_e^{'} = \frac{2\pi\varepsilon l}{\ln\left[\frac{(2l)}{d}\sqrt{\frac{(4s+l)}{(4s+3l)}}\right]} \quad (2)$$

l = length of cylinder (m)

d = diameter of cylinder (m)

s = distance between cylinder-end to ground (m)

ε = permittivity of free space ($8.854*10^{-12}$ F/m)

For the design as of l, d, and s are 1 m, 0. 20 m, and 0.20 m respectively, the stray capacitance is equal to 28.825 pF.

2.3 High voltage capacitance

The 100 kV capacitive voltage divider is designed for high voltage test up to 110% of rated voltage, which is 110 kV. The polypropylene film capacitors of rating 0.01μF , 1600dc/650Vac are selected to use by connecting in parallel to obtain the capacitance as of 0.02μF . At 110% of rated voltage, the number of capacitors is equal to 110 kV/650Vac = 169.2 or 170 pair or 340 capacitors. However, the total 350 capacitors are designed as 14-paralleled capacitors in a row and each row is connected in series up to 25 rows as shown in Fig. 4. Thus, the high voltage capacitance C_1 is 114.285 pF.

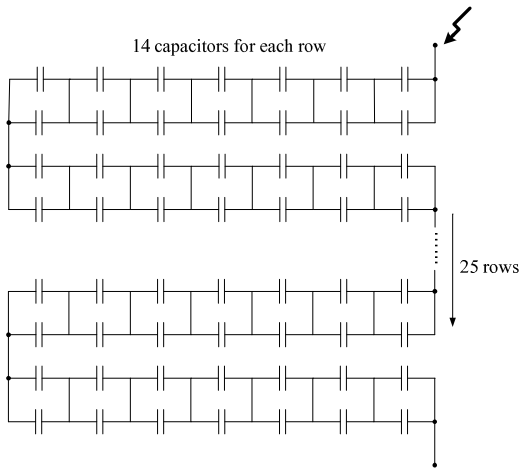

Fig. 4. Layout for HV Capacitance

2.4 Low voltage capacitance

The scale factor is designed as 1000:1. By using the formula of capacitive voltage divider in Eq. (1), the low voltage capacitance C_2 is 114.285*1000 pF = 0.114285 μF. Thus, 12-capacitors as of 0.01 μF are connected in parallel to obtain 0.12 μF. At the low voltage or output terminal the matching resistor of 50 Ω, which is equal to the surge impedance of coaxial cable, is connected to avoid the reflection of voltage wave.

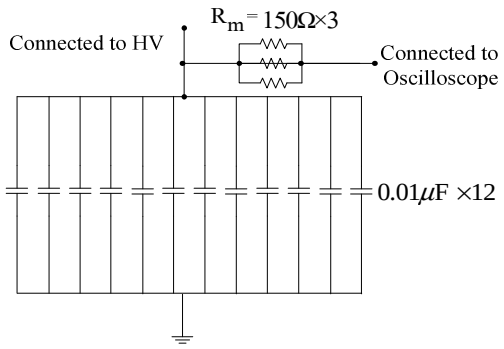

Fig. 5. Layout for LV Capacitance

3. EXPERIMENTAL SETUP

The acceptance tests on capacitive voltage divider are as follows.

3.1 Components measurement

The circuit in Fig. 6 is used to measure the resistance or capacitance by using RLC meter in order to compare the actual value with the designed value.

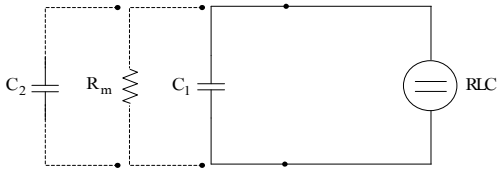

Fig. 6. Components of Measurement Circuit.

3.2 Withstand Voltage Test

A capacitor divider shall pass a dry withstand voltage test performed with a voltage of the required frequency or shape at a level of 110% of the rated measuring voltage. The procedure of withstand voltage tests is described in IEC 60-1 [3]. The equivalent circuit is given in Fig. 7.

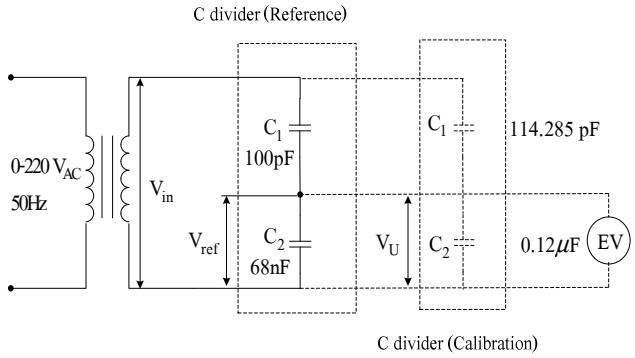

Fig. 7. Equivalent Testing Circuit at Rated 100 kV_{rms}

3.3 Determination of the Scale Factor

The circuit in Fig. 7 is used to determine the scale factor, which is calculated for the ratio of V_{in} and V_U. The designed value of scale factor is 1000:1.

3.4 Linearity Test

Using Fig. 7, values of the scale factor of the measuring system shall be measured at the minimum and maximum of the operating voltages and at three approximately equally spaced voltage or current between these extremes. These five values shall not differ by more than ±1% from their mean value.

3.5 Stability Test

Stability of the capacitor divider and the measurement system shall not vary by more than ±1% for the ranges of the ambient temperature and clearances given in the record of performance. The measuring instruments in Fig. 7 shall comply with the requirements of class 0.5 of IEC 51 [4] or shall be tested according to this standard if a peak voltmeter is used, its uncertainty shall be within ±1%.

4. EXPERIMENTAL RESULTS

The AC high voltage test circuit of rated 100 kV_{rms} is given in Fig. 8.

Fig. 8. Testing Circuit of Rated Voltage 100 kV_{rms}

This capacitive voltage divider was filled by gas insulation as air, N_2 and SF_6 for each test. The test procedures were followed the IEC 60060 - 2 (1994) standard.

Air-Insulated Capacitive Voltage Divider

In this test, air was filled in the cylinder of C_1 as gas insulation. However before any tests, the electrical value of the divider element must be measured. The results are presented in Table 2. The measured values show that the scale factor is 926:1 (113.000 pF/0.122 μF). The factors as capacitances and resistance are similar for N_2 and SF_6-insulation.

Table 2. Components Measurement

Component	Designed Value	Measured Value	% Error
C_1	114.285 pF	113.000 pF	1.12%
C_2	0.12 μF	0.122 μF	1.67%
R_m	50 Ω	49.93 Ω	0.14%

The pressure of air-insulation can be increased upto 2-bars in the cylinder. Actually for withstand test, the withstand voltage should rise up to 110 kV. However due to the poor dielectric withstand voltage of the air, there was an occurrence of corona discharge when the high voltage input was increased to nearly 30 kV. Then the withstand voltage test was stopped at that point to avoid electrical breakdown at higher voltage. The results show in Table 3. The divider can be operated against 30 kV for 60 second long.

Table 3. Withstand Test for Air-Insulated Voltage Divider

No.	Test Voltage (kV_{AC})	Time (Sec)	Result
1	30.18	60	Passed
2	30.06	60	Passed
3	30.04	60	Passed

The scale factor tests were performed at only 20 and 30 kV levels to avoid the corona discharge. The scale factors from the measurement shown in Table 4 are slightly different from the designed value as 1000:1. These result from the high and low voltage capacitors.

Table 4. Scale Factor Test for Air-Insulated Voltage Divider

No.	20 kV		30 kV	
	V_{in} (kV_{AC})	V_U (V_{AC})	V_{in} (kV_{AC})	V_U (V_{AC})
1	20.19	20.2	30.05	30.5
2	20.12	20.1	30.00	30.3
3	20.13	20.1	30.11	30.4
4	20.12	20.1	30.13	30.4
5	20.14	20.1	30.07	30.3
6	20.14	20.1	30.11	30.3
7	20.13	20.1	30.16	30.3
8	20.08	20.0	30.18	30.4
9	20.10	19.9	30.06	30.2
10	20.03	20.0	30.04	30.2
Avg.	20.11	20.07	30.09	30.33
Scale Factor	1001.9 :1		992.0 : 1	
% Error	0.19%		-0.8%	

The linearity test was also taken up to only 40 kV to avoid corona discharge. The results in Table 5 show that the average voltage ratio is 1.013. The upper limit for standard acceptance is (1+0.01)×1.013 =1.023 while the lower limit is (1-0.01)×1.013=1.002.

Table 5. Linearity Test for Air-Insulated Voltage Divider

V_{in} (kV_{AC})	V_{ref} (V_{AC})	V_U (V_{AC})	$\frac{V_U}{V_{ref}}$
10.12	10.12	10.3	1.017
20.03	20.03	20.4	1.018
30.03	30.03	30.6	1.018
40.04	40.04	40.0	0.999
Stop due to corona discharge			
Average			1.013

The voltage ratios were plotted in Fig. 9. The results show that only at 40 kV the voltage ratio exceeds the boundary.

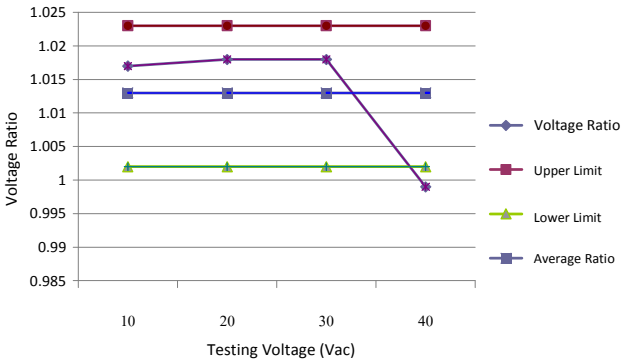

Fig. 9. Linearity for Air-Insulated Voltage Divider

For stability test, the test voltage of 30 kV was applied to stress the divider for 10 times. The mismatches of voltages were within ±3% as given in Table 6. Thus, it is acceptable up to the voltage 30 kV.

Table 6. Stability Test for Air-Insulated Voltage Divider

No.	V_{ref} (V_{AC})	V_U (V_{AC})	$\frac{V_U - V_{ref}}{V_{ref}} \times 100\%$
1	30.05	30.5	1.497%
2	30.00	30.3	1.000%
3	30.11	30.4	0.963%
4	30.13	30.4	0.896%
5	30.07	30.3	0.764%
6	30.11	30.3	0.631%
7	30.16	30.3	0.464%
8	30.18	30.4	0.728%
9	30.06	30.2	0.465%
10	30.04	30.2	0.532%
Average	30.09	30.33	0.794%

Nitrogen-Insulated Capacitive Voltage Divider

For withstand voltage test, the Nitrogen gas was pressured up to 2-bars in the cylinder. The corona discharge occurred when the high voltage input was raised to 80 kV. This corona discharge voltage was higher because of the better dielectric withstand voltage of Nitrogen gas than the air. When the corona inception voltage was known, the withstand voltage test was limited at 90 kV. The results of withstand voltage are shown in Table 7. The divider can be properly operated against the voltage of 90 kV for 60 second long without any damage.

Table 7. Withstand Test for N_2-Insulated Voltage Divider

No.	Test Voltage (kV_{AC})	Time (Sec)	Result
1	90.21	60	Passed
2	90.14	60	Passed
3	90.23	60	Passed

The scale factor tests were done at only 60 and 90 kV levels due to the corona at 90 kV. The scale factors from the measurement in Table 8 are slightly different from the designed value.

Table 8. Scale Factor Test for N_2-Insulated Voltage Divider

No.	60 kV		90 kV	
	V_{in} (kV_{AC})	V_U (V_{AC})	V_{in} (kV_{AC})	V_U (V_{AC})
1	60.05	60.5	90.04	90.4
2	60.13	60.6	90.07	90.4
3	60.09	60.6	90.17	90.6
4	60.17	60.7	90.05	90.4
5	60.05	60.6	90.1	90.4
6	60.01	60.5	90.08	90.5
7	60.01	60.4	90.02	90.3
8	60.05	60.5	90.14	90.5
9	60.04	60.5	90.15	90.5
10	60.16	60.7	90.08	90.4
Avg.	60.07	60.56	90.09	90.44
Scale Factor	991.9:1		996.1:1	
% Error	-0.0081		-0.0039	

The linearity test was also performed up to 90 kV due to the corona inception. The results were presented in Table 9. The average voltage ratio is 1.000. The upper limit for standard acceptance is (1+0.01)×1.000 =1.010 while the lower limit is (1-0.01)×1.000=0.990. The voltage ratios were plotted in Fig. 10. It shows that only at 10 kV the voltage ratio exceeds the boundary. At one voltage level of 10 kV only, less than five times out of ten times of the test the results are out of the boundary. Therefore, this divider is acceptable.

Table 9. Linearity Test for N_2-Insulated Voltage Divider

V_{in} (kV_{AC})	V_{ref} (V_{AC})	V_U (V_{AC})	$\frac{V_U}{V_{ref}}$
10.05	10.05	9.9	0.985
20.06	20.06	19.9	0.992
30.06	30.06	30.0	0.998
40.13	40.13	40.3	1.004
50.14	50.14	50.5	1.007
60.17	60.17	60.7	0.998
70.11	70.11	70.7	1.008
80.14	80.14	80.6	1.005
90.01	90.01	90.4	1.004
Stop due to corona discharge			
Average		1.000	

For stability test was performed 10 times at 90 kV, the mismatches of voltages given in Table 6 were within ±3%. Thus, it is acceptable up to the voltage of 90 kV.

SF6-Insulated Capacitive Voltage Divider

Because the test transformer was designed to operate up to 100 kV rms. maximum, the 110 % test was not possible. Thus the scale factor tests were done at only 50 and 100 kV levels. The scale factors from the measurement in Table 11 are slightly different from the designed value.

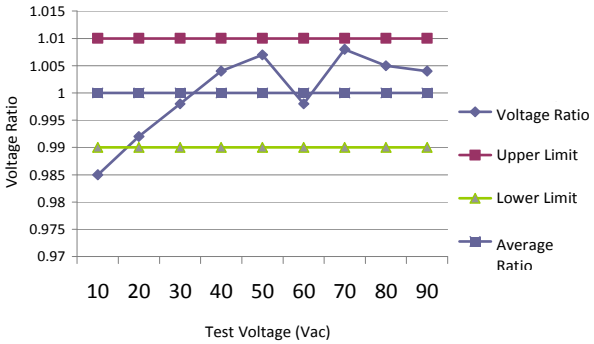

Fig. 10. Linearity for N_2-Insulated Voltage Divider

Table 10. Stability Test for N_2-Insulated Voltage Divider

No.	V_{in} (kV_{AC})	V_{ref} (V_{AC})	V_U (V_{AC})	$\frac{V_U - V_{ref}}{V_{ref}} \times 100\%$
1	90.04	90.04	90.4	0.399%
2	90.07	90.07	90.4	0.366%
3	90.17	90.17	90.6	0.476%
4	90.05	90.05	90.4	0.388%
5	90.10	90.10	90.4	0.332%
6	90.08	90.08	90.5	0.466%
7	90.02	90.02	90.3	0.311%
8	90.14	90.14	90.5	0.399%
9	90.15	90.15	90.5	0.388%
10	90.08	90.08	90.4	0.352%
Avg.	90.09	90.09	90.44	0.387%

Table 11. Scale Factor Test for SF_6-Insulated Voltage Divider

No.	50 kV		100 kV	
	V_{in} (kV_{AC})	V_U (V_{AC})	V_{in} (kV_{AC})	V_U (V_{AC})
1	50.15	50.1	100.2	101.5
2	50.15	50.1	100.1	101.4
3	50.02	49.9	100.2	101.5
4	50.05	50.0	100.0	100.9
5	50.10	50.0	100.1	101.2
6	50.12	50.1	100.0	100.7
7	50.12	50.0	100.0	100.8
8	50.01	49.9	100.1	101.0
9	50.01	50.0	100.1	101.9
10	50.08	50.0	100.2	101.0
Avg.	50.08	50.01	100.10	101.19
Scale Factor	1001.3 : 1		989.2 : 1	
% Error	1.3%		-1.08%	

Similar to the previous gases, SF_6-insulation was pressured up to 2-bars in the cylinder. The withstand voltage test was taken only up to 100 kV, which cannot reach 110 % of the designed voltage due to the limitation of the test transformer. However up to 100 kV, the

voltage divider worked properly without corona discharge, because the dielectric withstand voltage of SF_6 is better than the air or Nitrogen due to the electro-negative gas property of SF_6.

Table 12. Withstand Test for SF_6-Insulated Voltage Divider

No.	Test Voltage (kV_{AC})	Time (Sec)	Result
1	100.1	60	Passed
2	100.1	60	Passed
3	100.2	60	Passed

The linearity test was also taken up to 100 kV due to the limitation of the test transformer. The results show that the average voltage ratio is 0.997. The results were plotted in Fig. 10, which shows that only at 10 and 100 kV the voltage ratios exceed the boundary. Then only two out of ten times of tested voltages are out of the boundary. The divider is acceptable.

Table 13. Linearity Test for SF_6-Insulated Voltage Divider

$V_{in}(kV_{AC})$	V_{ref} (V_{AC})	V_U (V_{AC})	$\frac{V_U}{V_{ref}}$
10.11	9.9	0.979	-2.077%
20.02	19.8	0.989	-1.098%
30.11	29.9	0.993	-0.697%
40.11	40.0	0.997	-0.274%
50.05	50.1	1.000	0.099%
60.07	60.3	1.003	0.383%
70.03	70.3	1.003	0.385%
80.09	80.3	1.002	0.262%
90.09	90.0	0.999	-0.099%
100.1	101.4	1.012	1.298%
10.11	9.9	0.979	-2.077%
Stop due to limitation of the test transformer			
Average		0.997	

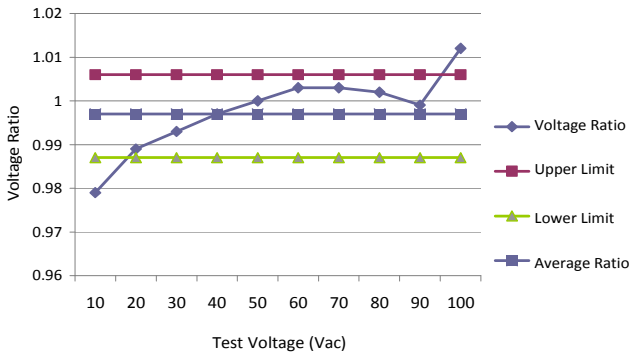

Fig. 11. Linearity for SF_6-Insulated Voltage Divider.

For stability test, the voltage up to 100 kV was performed. The calculated mismatches of voltages given in Table 14 were within ±3%. Thus, this voltage divider can reliably operate up to the voltage of 100 kV.

Table 14. Stability Test for SF_6-Insulated Voltage Divider

No.	V_{in} (kV_{AC})	V_U(V_{AC})	$\frac{V_U - V_{ref}}{V_{ref}} \times 100\%$
1	100.2	101.5	1.297%
2	100.1	101.4	1.298%
3	100.2	101.5	1.297%
4	100.0	100.9	0.900%
5	100.1	101.2	0.599%
6	100.0	100.7	0.700%
7	100.0	100.8	0.800%
8	100.1	101.0	0.899%
9	100.1	101.9	1.798%
10	100.2	101.0	0.798%
Averag	100.10	101.19	1.038%

Comparison between Air, N2 and SF6

In term of dielectric strength, the air-insulated voltage divider could operate up to 30 kV only due to the inception of corona. Thus, using of the air-insulation in the capacitive voltage divider yields the lowest operating voltage when compared with N_2 and SF_6 gas insulation. This is due to the poor dielectric property of the air.

Actually, the dielectric strength of the air and N_2 is not significantly different. However, the advantage of N_2 is that the contact erosion is less than the air under no O_2 condition. Comparison between N_2 and SF_6, when using N_2 there was a corona inception at 80 kV but no corona for SF_6 at 100 kV when both gases are pressurized at 2 bars. This means SF_6 has better dielectric strength than air and N_2.

5. CONCLUSION

A 100 kV capacitive voltage divider was designed, constructed, and tested. The experiments as components measurement, scale factor test, linearity test, withstand voltage test, and stability test are performed and reported. The tested results show that the capacitive divider can be properly operated as a measurement divider under the IEC 60060 – 2 (1994) standard. Due to withstand voltage, stability, and chemical properties, the SF_6 is proposed as the preferred insulation for this 100 kV capacitive voltage divider.

ACKNOWLEDGMENT

The authors gratefully acknowledge the Naresuan University for financial support and Mr. Nutthaphan Boonsaner for technical support.

REFERENCES

[1] IEC 60060-2 (1994). High voltage test techniques - Part 2: Measuring systems.

[2] Kuffel, E., Zaengl, W. S., and Kuffel, J. 2001. High voltage engineering: fundamentals, 2nd Edition, Butterworth–Heinemann.

[3] IEC 60 –1 (1989). High-voltage test technique part 1: General definitions and test requirements.

[4] IEC 51-1 (1984). Direct acting indicating analogue electrical measuring instruments and their accessories.

Augmented Lagrange Hopfield for Real Power Loss Minimization in Power Systems

Dieu Ngoc Vo, Hoang Khanh Cap Le, and Khai Phuc Nguyen

Abstract*— *This paper proposes an augmented Lagrange Hopfield network (ALHN) for solving real loss minimization in power systems. The proposed ALHN is a conventional continuous Hopfield network with its energy function based on augmented Lagrange function. Moreover, the proposed method is a recurrent network with parallel processing which leads to fast convergence for large-scale problems. In the considered problem, the real power loss is determined using B-coefficients. The proposed method has been tested on the IEEE 14-bus, 30-bus, and 57-bus systems. The obtained results have indicated that the proposed ALHN can obtain better optimal solutions than particle swarm optimization (PSO) in a very fast manner. Therefore, the proposed ALHN can be implemented for solving the real power minimization problem in power systems.

***Keywords*— Augmented Lagrange Hopfield network, real power loss minimization, neural network, power flow.**

1. INTRODUCTION

In modern power systems, the improvement of operation has become more important due its contribution to the enhancement of power system efficiency. The minimization of real power losses in power systems is also very important because it can lead to a more economic operation of a power system. Once real power loss in power systems is minimized, the electric power is more efficiently consumed [1]. For real power loss minimization, the existing generation and transmission systems can be efficiently utilized without building new systems. Therefore, the objective of the real power loss minimization is to determine power generation of power plants so as the total real power loss in power systems is minimized to save cost of loss satisfying power constraint and generator limits.

Due to its importance, the problem of power loss minimization has been investigated by several researches [2-5]. In [2], the power loss in the system is calculated using B-coefficients and verified with traditional RI^2 or differential power methods based on the solution of power flow by Newton-Raphson method. In the proposed method, the voltage control using capacitor bank or transformer tap changer will be done to improve voltage level while power loss minimized. In [3], a hybrid particle swarm optimization is implemented for loss reduction study. The proposed application in this paper is the use of a developed optimal power flow based on loss minimization function including two steps. The first is to determine the critical area of the power system under the point of view of voltage instability, and the second is to calculate the amount of shunt reactive power compensation that takes place in each bus by particle swarm optimization method. In [4], meta-heuristic search methods such as bacteria foraging algorithm, conventional algorithm, and differential genetic algorithm have been implemented for transmission loss minimization. The active loss minimization problem has been solved by a predictor–corrector modified barrier approach. In this proposed approach, the inequality problem constraints are transformed into equalities by introducing positive auxiliary variables perturbed by the barrier parameter and treated by the modified barrier method.

In this paper, an augmented Lagrange Hopfield network (ALHN) is proposed for solving real loss minimization in power systems. The proposed ALHN is a conventional continuous Hopfield network with its energy function based on augmented Lagrange function. Moreover, the proposed method is a recurrent network with parallel processing which leads to fast convergence for large-scale problems. In the considered problem, the real power loss is determined using B-coefficients. The proposed method has been tested on the IEEE 14-bus, 30-bus, and 57-bus systems. The obtained results are compared to those particle swarm optimization method.

2. PROBLEM FORMULATION

Mathematically, the real power loss minimization is formulation as follows:

The objective is to minimize total real power loss:

$$\text{Min } P_{loss} \tag{1}$$

subject to:

- Real power balance

$$\sum_{i=1}^{N} P_{gi} = P_D + P_{loss} \tag{2}$$

- Ramp rate constraint

The authors are with Department of Power Systems, Ho Chi Minh City University of Technology, 268 Ly Thuong Kiet str., 10th dist., HCMC, Vietnam. Email: vndieu@hcmut.edu.vn (D.N. Vo).

$$P_{gi} - P_{gi}^0 \le UR_i \text{, as power increases} \quad (3)$$

$$P_{gi}^0 - P_{gi} \le DR_i \text{, as power decreases} \quad (4)$$

- Generator limits

$$P_{gi,\min} \le P_{gi} \le P_{gi,\max} \quad (5)$$

where

N : number of generators
P_{loss} : total real power loss
P_{gi} : real power output of generator i
$P_{gi,max}$: maximum real power output of generator i
$P_{gi,min}$: minimum real power output of generator i
P^0_{gi} : initial real power output of generator i
P_D : total power system demand

3. AUGMENTED LAGRANGE HOPFIELD NETWORK IMPLEMENTATION

For implementation in ALHN, the real power loss in (1) is calculated using Kron's formula [6]:

$$P_{loss} = \sum_{i=1}^{N}\sum_{j=1}^{N} P_{gi} B_{ij} P_{gj} + \sum_{i=1}^{N} B_{0i} P_{gi} + B_{00} \quad (6)$$

where B_{ij}, B_{0i}, and B_{00} are the B-coefficients for real power loss.

The augmented Lagrange function is formulated for the problem:

$$L = \sum_{i=1}^{N}\sum_{j=1}^{N} P_{gi} B_{ij} P_{gj} + \sum_{i=1}^{N} B_{0i} P_{gi} + B_{00} + \lambda\left(P_D + P_{loss} - \sum_{i=1}^{N} P_{gi}\right) + \frac{1}{2}\beta\left(P_D + P_{loss} - \sum_{i=1}^{N} P_{gi}\right)^2 \quad (7)$$

where λ and β are Lagrange multiplier and penalty factor, respectively.

The energy function of ALHN is formulated based on the augmented Lagrange function as follows:

$$E = \sum_{i=1}^{N}\sum_{j=1}^{N} V_{gi} B_{ij} V_{gj} + \sum_{i=1}^{N} B_{0i} V_{gi} + B_{00} + V_\lambda\left(P_D + P_{loss} - \sum_{i=1}^{N} V_{gi}\right) + \frac{1}{2}\beta\left(P_D + P_{loss} - \sum_{i=1}^{N} V_{gi}\right)^2 + \int_0^{V_{gi}} g^{-1}(V)\,dV \quad (8)$$

where V_{gi} is the output of continuous neuron i representing power output P_{gi} of generator i, V_λ is the output of the multiplier neuron representing the Lagrange multiplier λ, and $g^{-1}(V)$ is the inverse function of sigmoid function of continuous neurons.

In (8), the sums of integral terms are Hopfield terms where their global effect is a displacement of solutions toward the interior of the state space [7].

The dynamics of the neurons are defined by:

$$\frac{dU_{gi}}{dt} = -\frac{\partial E}{\partial V_{gi}} = -\left\{\begin{array}{l}\left(\sum_{j=1}^{N} 2B_{ij}P_{gi} + B_{0i}\right) \\ + \left[V_\lambda + \beta\left(P_D + P_{loss} - \sum_{i=1}^{N} V_{gi}\right)\right] \\ \times\left[\left(\sum_{j=1}^{N} 2B_{ij}P_{gi} + B_{0i}\right) - 1\right] + U_{gi}\end{array}\right\} \quad (9)$$

$$\frac{dU_\lambda}{dt} = +\frac{\partial E}{\partial V_\lambda} = P_D + P_{loss} - \sum_{i=1}^{N} P_{gi} \quad (10)$$

where U_{gi} and U_λ are the inputs of continuous and multiplier neurons, respectively.

The inputs of neurons at iteration n are updated by:

$$U_{gi}^{(n)} = U_{gi}^{(n-1)} - \alpha_i \frac{\partial E}{\partial V_{gi}} \quad (11)$$

$$U_\lambda^{(n)} = U_\lambda^{(n-1)} + \alpha_\lambda \frac{\partial E}{\partial V_\lambda} \quad (12)$$

where α_i and α_λ are updating step size of continuous and multiplier neurons, respectively.

The outputs of continuous neurons are calculated using a sigmoid function:

$$V_{gi} = g(U_{gi}) = \left(\frac{P_{gi,high} - P_{gi,low}}{2}\right)[1 + \tanh(\sigma U_{gi})] + P_{gi,low} \quad (13)$$

where

$$P_{i,high} = \min\left\{P_{gi,\max}, P_{gi}^0 + UR_i\right\} \quad (14)$$

$$P_{i,low} = \max\left\{P_{gi,\min}, P_{gi}^0 - DR_i\right\} \quad (15)$$

The output of the multiplier neuron is calculated using a transfer function:

$$V_\lambda = g(U_\lambda) = U_\lambda \quad (16)$$

Selection of parameters

In the ALHN, the parameters have to be predetermined including sigmoid function slope, updating step sizes for neurons and penalty factors for augmented Lagrange function. By experiments, the values of sigmoid function slope and penalty factors are fixed at 100 and 0.001, respectively. The values of the others will vary depending on the data of considered problem. It is observed that the larger the value of updating step sizes the closer the discrete system behavior, producing values at the upper and lower limits of each neuron. On the contrary, the smaller the value of updating step sizes the slower convergence of the network.

Initialization

In the proposed ALHN, all neurons need to be initialized. For the continuous neurons, their initial outputs are determined:

$$V_{gi}^{(0)} = P_D \frac{P_{gi,\max}}{\sum_{i=1}^{N} P_{gi,\max}} \quad (17)$$

and the output of the multiplier neuron is initialized by:

$$V_{\lambda}^{(0)} = -\frac{\sum_{j=1}^{N} 2B_{ij}P_{gj} + B_{0i}}{\sum_{j=1}^{N} 2B_{ij}P_{gj} + B_{0i} - 1} \quad (18)$$

The inputs of all neurons are determined based on their outputs using the inverse function of sigmoid function for continuous neurons and transfer function for the multiplier neuron.

The proof of convergence and the explanation of the proposed ALHN method are given in [8].

Stopping criteria

The algorithm of ALHN will be terminated when either the maximum error Err_{max} including constraint error and iterative error is lower than a pre-specified tolerance ε or maximum number of iterations N_{max} is reached.

Overall procedure

Overall algorithm of ALHN for solving the problem is as follows:

Step 1: Solve power flow problem by Newton-Raphson to determine B-coefficients.

Step 2: Select parameters for the neural network.

Step 3: Initialize outputs of all neurons and calculate their corresponding inputs.

Step 4: Set n = 1.

Step 5: Calculate dynamics of neurons using (9)-(10).

Step 6: Update inputs of neurons using (11), (12).

Step 7: Calculate corresponding outputs of neurons using (13) and (16).

Step 8: Solve power flow problem by Newton-Raphson to determine B-coefficients

Step 7: If $Err_{max} > \varepsilon$ and $n < N_{max}$, $n = n + 1$ and return to Step 4. Otherwise, stop.

4. NUMERICAL RESULTS

The proposed ALHN has been tested on the IEEE 14-bus, 30-bus, and 57-bus systems. The data for these test systems are given in [9-10]. For result comparison, the PSO method [11] has been also implemented for solving these systems. The algorithms of the methods are coded in Matlab and run on a 1.6 GHz Intel PC. For obtaining power flow solution, the Matpower toolbox [10] has been used. For stopping criteria of the ALHN algorithm, the maximum error and maximum number of iterations are set to 10^{-3} and 2500, respectively.

The IEEE 14-bus system: The system includes 14 buses and 20 branches, in which there five generation buses and three transformer branches. The total real power demand of the system is 259 MW. The diagram of this system is given in Appendix. The result comparison from ALHN and PSO is given in Table 1 and the energy characteristic of the ALHN for the system is given in Fig. 1.

The IEEE 30-bus system: The system includes 30 buses and 41 branches, in which there six generation buses and four transformer branches. The total real power demand of the system is 283.4 MW. The diagram of this system is given in Appendix. The result comparison from ALHN and PSO is given in Table 2 and the energy characteristic of the ALHN for the system is given in Fig. 2.

Table 1. Result comparison for the IEEE 14-bus system

			ALHN	PSO
Bus	$P_{i,min}$ (MW)	$P_{i,max}$ (MW)	P_i (MW)	P_i (MW)
1	50	200	67.0495	97.5839
2	20	80	80	64.1423
3	15	50	50	43.8667
6	10	30	30	26.0951
8	10	35	35	31.2324
P_L (MW)			3.0486	3.9204
CPU (s)			0.75	4.79

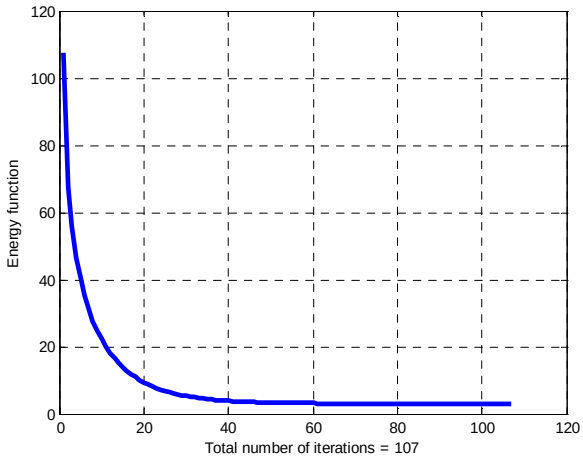

Fig. 1. Energy function of ALHN for the IEEE 14-bus system.

Table 2. Result comparison for the IEEE 30-bus system

			ALHN	PSO
Bus	$P_{i,min}$ (MW)	$P_{i,max}$ (MW)	P_i (MW)	P_i (MW)
1	50	200	51.9894	95.9628
2	20	80	80	60.8501
5	15	50	50	48.3410
8	10	35	35	30.0364
11	10	30	30	25.5737
13	20	40	40	27.2553
P_L (MW)			3.5886	4.6193
CPU (s)			1.14	5.60

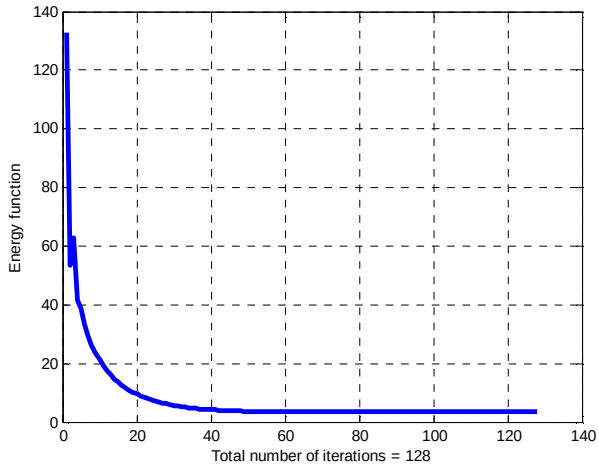

Fig. 2. Energy function of ALHN for the IEEE 30-bus system.

The IEEE 57-bus system: The system includes 57 buses and 80 branches, in which there seven generation buses and fifteen transformer branches. The total real power demand of the system is 1250.8 MW. The diagram of this system is given in Appendix. The result comparison from ALHN and PSO is given in Table 3 and the energy characteristic of the ALHN for the system is given in Fig. 3.

Based on the result comparison given in Tables 1, 2, and 3, the proposed ALHN can obtain better solutions than the PSO method for the all test systems. Moreover, the proposed ALHN also obtain the solutions much faster than the PSO method for all systems. Therefore, the proposed ALHN is more efficient than the PSO method for solving the problem.

Table 3. Result comparison for the IEEE 57-bus system

			ALHN	PSO
Bus	$P_{i,min}$ (MW)	$P_{i,max}$ (MW)	P_i (MW)	P_i (MW)
1	200	600	200	212.9463
2	30	150	30	30
3	30	140	107.2187	96.2084
6	20	100	99.9528	100
8	120	550	266.5468	264.5912
9	20	150	150	150
12	100	410	410	410
P_L (MW)			12.9175	12.9458
CPU (s)			2.46	6.93

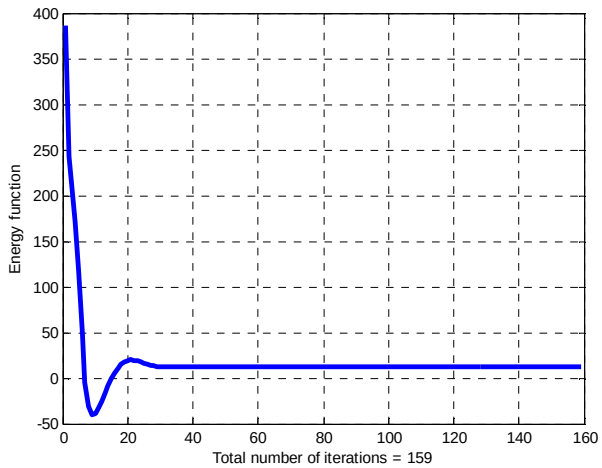

Fig. 3. Energy function of ALHN for the IEEE 14-bus system.

5. CONCLUSION

In this paper, the ALHN has been efficiently implemented for solving the real power loss minimization problem in power systems. The ALHN method is a simple and very easy implementation on optimization problems in power systems. The proposed uses augmented Lagrange function for handling equality constraints of the problem while the sigmoid function of continuous neurons can properly handle inequality constraints of the problem. In addition, the ALHN method is based on the parallel processing of neural network which leads to very fast convergence. The proposed ALHN has been tested on the IEEE 14-bus, 30-bus, and 57-bus systems and the obtained results have indicated that the proposed ALHN is more efficient than PSO in terms of total power loss and computational time. Therefore, the proposed ALHN could be applicable for solving the real power loss minimization in power systems.

REFERENCES

[1] Lukman, D., Blackburn, T.R. and Walshe, K. (2000). Loss minimization in industrial power system operation. *Proc. of the Australasian Universities Power Engineering Conference (AUPEC'94)*, Brisbane, Australia.

[2] Lukman, D. and Blackburn, T.R. (2001). Modified algorithm of load flow simulation for loss minimization in power systems. *Proc. of the Australasian Universities Power Engineering Conference (AUPEC-2001)*, Perth, Australia.

[3] Esmin, A..A.A, Lambert-Torres, G., and de Souza, A.C.Z. 2005. A hybrid particle swarm optimization applied to loss power minimization. *IEEE Trans. Power Systems*, 20(2): 859-866.

[4] Mishra, S., Redely, G.D., Rao, P.E. and Santosh, K. (2007). Implementation of new evolutionary techniques for transmission loss reduction. *IEEE Congress on Evolutionary Computation* (CEC 2007), Singapore.

[5] de Sousaa, V.A., Baptistab, E.C., and da Costa, G.R.M. 2009. Loss minimization by the predictor–corrector modified barrier approach. *Electric Power Systems Research*, 79 (5): 803-808.

[6] Wood, A.J. and Wollenberg, B.F. 1996. Power system generation, operation and control, 2nd ed., New York: John Wiley.

[7] van den Berg, J. and Bioch, J.C. (1993). Constrained optimization with a continuous Hopfield-Lagrange model. Technical report EUR-CS-93-10, Erasmus University Rotterdam, Comp. Sc. Dept., Faculty of Economics.

[8] Dieu, V. N. and Ongsakul, W. 2006. Enhanced augmented Lagrangian Hopfield network for unit commitment. *IEE Proc. Generat. Transm. Distrib.*, 153(6): 624-632.

[9] Dabbagchi, I. and Christie, R. (1993). Power systems test case archive. *University of Washington*. Retrieved Feb. 20, 2011, from http://www.ee.washington.edu/research/pstca/.

[10] Zimmerman, R.D.; Murillo-Sánchez; C.E. and Thomas, R.J. (2011). MATPOWER steady-state operations, planning and analysis tools for power systems research and education. *IEEE Trans. Power Systems*, 26(1): 12-19.

[11] Kennedy, J. and Eberhart, R. (1995). Particle swarm optimization. *Proc. IEEE Conf. Neural Networks* (ICNN'95), Perth, Australia, vol. IV: 1942-1948.

APPENDIX

The diagram of the IEEE 14-bus, 30-bus and 57-bus systems are given in Figs. 4, 5, and 6, respectively.

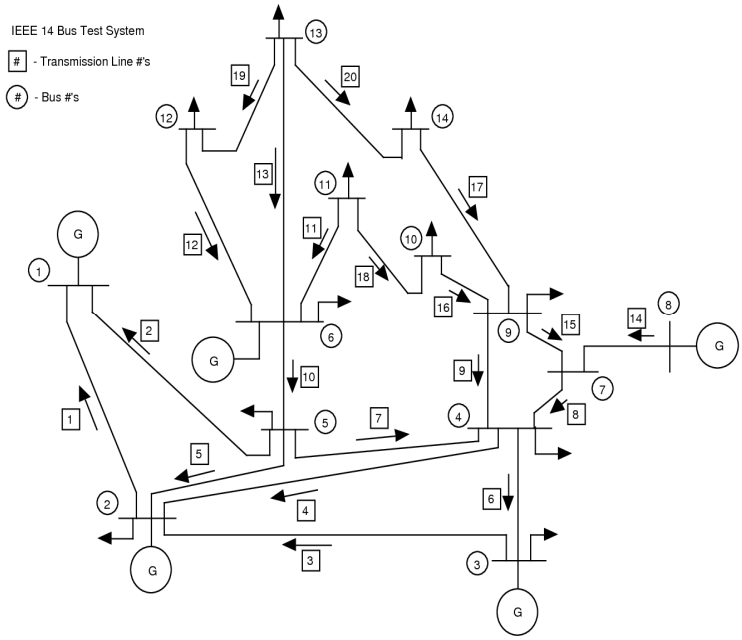

Fig. 4. The IEEE 14-bus system.

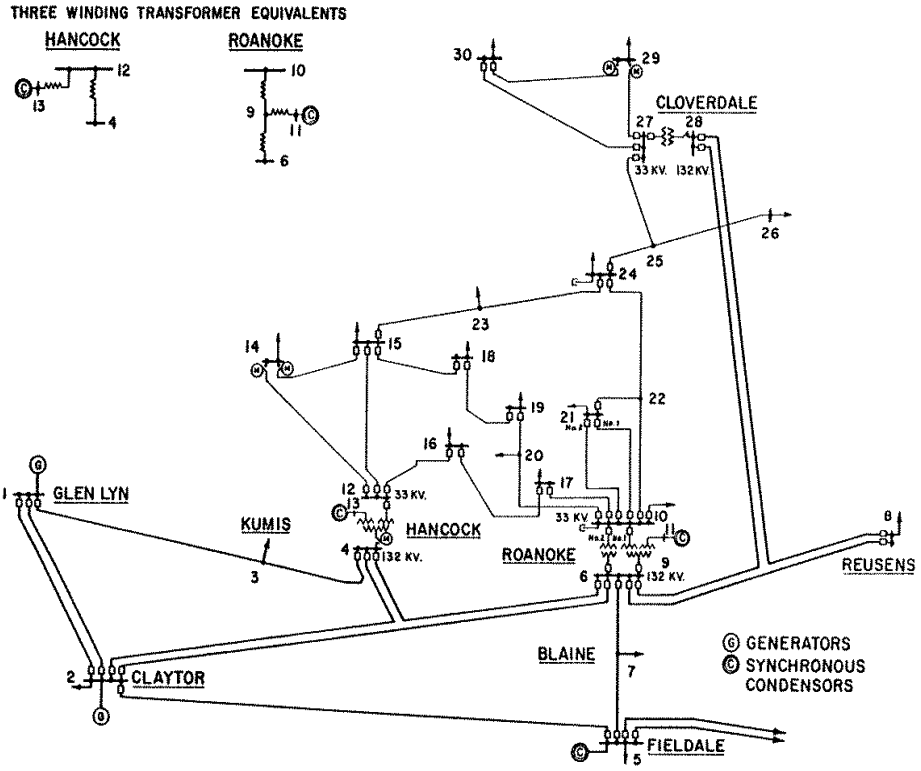

Fig. 5. The IEEE 30-bus system.

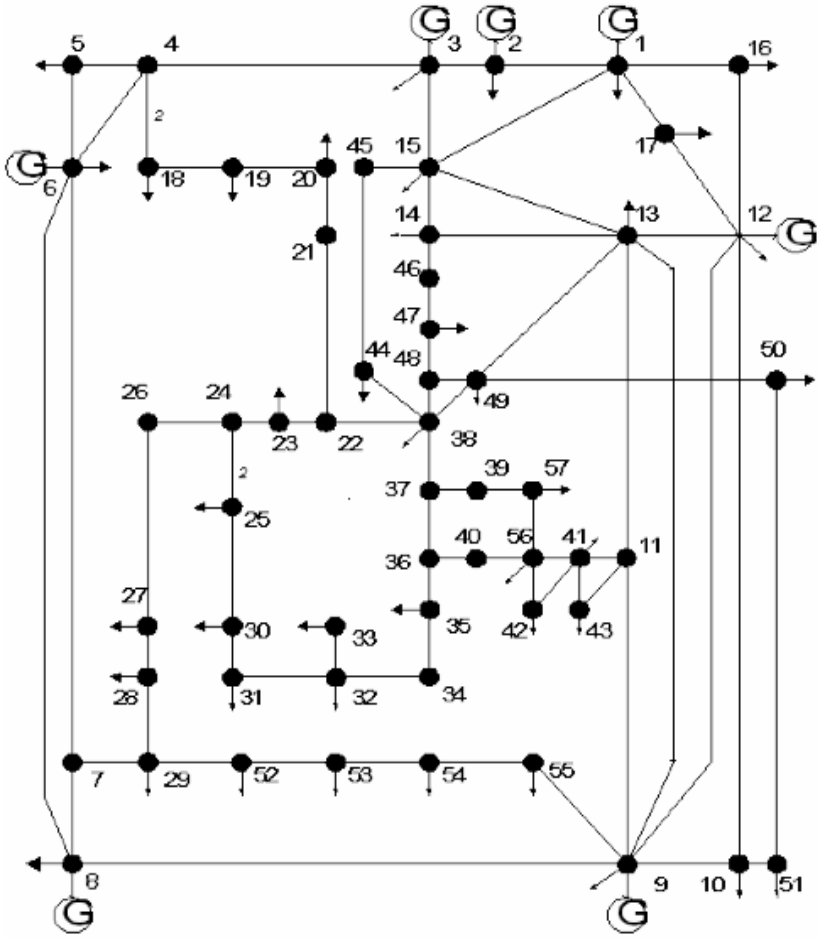

Fig. 6. The IEEE 57-bus system.

GMSARN International Journal
NOTES FOR AUTHORS

Editorial Policy

In the Greater Mekong Subregion, home to about 250 million people, environmental degradation - including the decline of natural resources and ecosystems will definitely impact on the marginalized groups in society - the poor, the border communities especially women and children and indigenous peoples. The complexity of the challenges are revealed in the current trends in land and forest degradation and desertification, the numerous demands made on the Mekong river - to provide water for industrial and agricultural development, to sustain subsistence fishing, for transport, to maintain delicate ecological and hydrological balance, etc., the widespread loss of biological diversity due to economic activities, climate change and its impacts on the agricultural and river basin systems, and other forms of crises owning to conflicts over access to shared resources. The *GMSARN International Journal* is dedicated to advance knowledge in energy, environment, natural resource management and economical development by the vigorous examination and analysis of theories and good practices, and to encourage innovations needed to establish a successful approach to solve an identified problem.

The *GMSARN International Journal* is a quarterly journal published by GMSARN in March, June, September and December of each year. Papers related to energy, environment, natural resource management, and economical development are published. The papers are reviewed by world renowned referees.

Preparation Guidelines

1. The manuscript should be written in English and the desired of contents is: Title, Author's name, affiliation, and address; Abstract, complete in itself and not exceeding 200 words; Text, divided into sections, each with a separate heading; Acknowledgments; References; and Appendices. The standard International System of Units (SI) should be used.

2. Illustrations (i.e., graphs, charts, drawings, sketches, and diagrams) should be submitted on separate sheets ready for direct reproduction. All illustrations should be numbered consecutively and given proper legends. A list of illustrations should be included in the manuscript. The font of the captions, legends, and other text in the illustrations should be Times New Roman. Legends should use capital letters for the first letter of the first word only and use lower case for the rest of the words. All symbols must be italicized, e.g., α, θ, Q_{wt}. Photographs should be black and white glossy prints; but good color photographs are acceptable.

3. Each reference should be numbered sequentially and these numbers should appear in square brackets in the text, e.g. [1], [2, 3], [4]–[6]. All publications cited in the text should be presented in a list of full references in the Reference section as they appear in the text (not in alphabetical order). Typical examples of references are as follows:

   - **Book references** should contain: name of author(s); year of publication; title; edition; location and publisher. Typical example: [2] Baker, P.R. 1978. Biogas for Cooking Stoves. London: Chapman and Hall.
   - **Journal references** should contains: name of author(s); year of publication; article title; journal name; volume; issue number; and page numbers. For example: Mayer, B.A.; Mitchell, J.W.; and El-Wakil, M.M. 1982. Convective heat transfer in veetrough liner concentrators. Solar Energy 28 (1): 33-40.
   - **Proceedings reference** example: [3] Mayer, A. and Biscaglia, S. 1989. Modelling and analysis of lead acid battery operation. Proceedings of the Ninth EC PV Solar Conference. Reiburg, Germany, 25-29 September. London: Kluwer Academic Publishers.
   - **Technical paper** reference example: [4] Mead, J.V. 1992. Looking at old photographs: Investigating the teacher tales that novice teachers bring with them. Report No. NCRTL-RR-92-4. East Lansing, MI: National Center for Research on Teacher Learning. (ERIC Document Reproduction Service No. ED346082).
   - **Online journal** reference example: [5] Tung, F. Y.-T., and Bowen, S. W. 1998. Targeted inhibition of hepatitis B virus gene expression: A gene therapy approach. Frontiers in Bioscience [On-line serial], 3. Retrieved February 14, 2005 from http://www.bioscience.org/1998/v3/a/tung/a11-15.htm.

4. Manuscript can be uploaded to the website or sent by email. In case of hard copy, three copies of the manuscript should be initially submitted for review. The results of the review along with the referees' comments will be sent to the corresponding author in due course. At the time of final submission, one copy of the manuscript and illustrations (original) should be submitted with the diskette. Please look at the author guide for detail.

GMSARN Members

Asian Institute of Technology

Guangxi University

Hanoi University of Technology

Ho Chi Minh City University of Technology

Institute of Technology of Cambodia

Khon Kaen University

Kunming University of Science and Technology

National University of Laos

Royal University of Phnom Penh

Thammasat University

Yangon Technological University

Yunnan University

Associate Members

Chulalongkorn University

Mekong River Commission

Nakhon Phanom University

Ubon Rajathanee University

Published by the **Greater Mekong Subregion Academic and Research Network (GMSARN)**
c/o Asian Institute of Technology (AIT)
P.O. Box 4, Klong Luang
Pathumthani 12120, Thailand
Tel: (66-2) 524-5437; Fax: (66-2) 524-6589
E-mail: gmsarn@ait.asia
Website: http://www.gmsarn.org